European Neuropsychopharmacology (2019) 29, 880–896

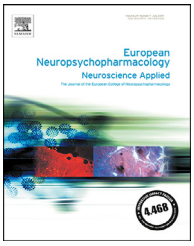

www.elsevier.com/locate/euroneuro

Risperidone administered during adolescence induced metabolic, anatomical and inflammatory/oxidative changes in adult brain: A PET and MRI study in the maternal immune stimulation animal model

Marta Casquero-Veiga[a,b], David García-García[c,i], Karina S. MacDowell[b,g], Laura Pérez-Caballero[b,d,e], Sonia Torres-Sánchez[b,e,f], David Fraguas[b,h], Esther Berrocoso[b,d,e], Juan C. Leza[b,g], Celso Arango[b,h], Manuel Desco[a,c,b,j,*], María Luisa Soto-Montenegro[a,b]

[a] *Instituto de Investigación Sanitaria Gregorio Marañón, Madrid, Spain*
[b] *CIBER de Salud Mental (CIBERSAM), Madrid, Spain*
[c] *Department of Bioengineering and Aerospace Engineering, Universidad Carlos III de Madrid, Leganés, Spain*
[d] *Neuropsychopharmacology & Psychobiology Research Group, Psychobiology Area, Department of Psychology, Universidad de Cádiz, Puerto Real (Cádiz), Spain*
[e] *Instituto de Investigación e Innovación en Ciencias Biomédicas de Cádiz, INiBICA, Hospital Universitario Puerta del Mar, Cádiz, Spain*
[f] *Neuropsychopharmacology & Psychobiology Research Group, Universidad de Cádiz, Cádiz, Spain*
[g] *Department of Pharmacology & Toxicology, School of Medicine, Universidad Complutense (UCM), IIS Imas12, IUIN, Madrid, Spain*
[h] *Department of Child and Adolescent Psychiatry, Hospital General Universitario Gregorio Marañón, School of Medicine, Universidad Complutense (UCM), Madrid, Spain*
[i] *Facultad de Ciencia y Tecnología, Universidad Isabel I, Burgos, Spain*
[j] *Centro Nacional de Investigaciones Cardiovasculares, CNIC, Madrid, Spain*

Received 21 August 2018; received in revised form 30 April 2019; accepted 29 May 2019

*Corresponding author at: Laboratorio de Imagen. Medicina Experimental, Hospital General Universitario Gregorio Marañón, Dr. Esquerdo, 46. E-28007 Madrid. Spain.
E-mail address: desco@hggm.es (M. Desco).

https://doi.org/10.1016/j.euroneuro.2019.05.002

KEYWORDS
Schizophrenia;
FDG-PET;
Poly I:C;
Risperidone;
Dopamine antagonist;
Inflammation/
oxidonitrosative stress

Abstract
Inflammation and oxidative stress (IOS) are considered key pathophysiological elements in the development of mental disorders. Recent studies demonstrated that the antipsychotic risperidone elicits an antiinflammatory effect in the brain. We administered risperidone for 2-weeks at adolescence to assess its role in preventing brain-related IOS changes in the maternal immune stimulation (MIS) model at adulthood. We also investigated the development of volumetric and neurotrophic abnormalities in areas related to the HPA-axis. Poly I:C (MIS) or saline (Sal) were injected into pregnant Wistar rats on GD15. Male offspring received risperidone or vehicle daily from PND35-PND49. We studied 4 groups (8–15 animals/group): Sal-vehicle, MIS-vehicle, Sal-risperidone and MIS-risperidone. [^{18}F]FDG-PET and MRI studies were performed at adulthood and analyzed using SPM12 software. IOS and neurotrophic markers were measured using WB and ELISA assays in brain tissue. Risperidone elicited a protective function of schizophrenia-related IOS deficits. In particular, risperidone elicited the following effects: reduced volume in the ventricles and the pituitary gland; reduced glucose metabolism in the cerebellum, periaqueductal gray matter, and parietal cortex; higher FDG uptake in the cingulate cortex, hippocampus, thalamus, and brainstem; reduced NFκB activity and iNOS expression; and increased enzymatic activity of CAT and SOD in some brain areas. Our study suggests that some schizophrenia-related IOS changes can be prevented in the MIS model. It also stresses the need to search for novel strategies based on anti-inflammatory compounds in risk populations at early stages in order to alter the course of the disease.

1. Introduction

Schizophrenia is a chronic neuropsychiatric disorder that is considered the most severe expression of the psychosis spectrum syndrome. Recent studies showed that infection during pregnancy acts synergistically with other risk factors, thus increasing the risk of psychosis in offspring (Blomstrom et al., 2016). Furthermore, clinical and pre-clinical studies indicate that both neonates who will develop psychosis and adults with psychosis have deficiencies in innate immunity, suggesting that they are more vulnerable to infections (Gardner et al., 2013). Genetic and transcriptomic studies also support the contribution of immune activation to schizophrenia and psychosis (Ripke et al., 2013; Sanders et al., 2017; Schizophrenia Working Group of the Psychiatric Genomics, 2014). Moreover, predisposition to other environmental factors increases the sensitivity of some individuals to stress, thus contributing to immune activation and making them more vulnerable to developing psychosis under stressful circumstances (van Os et al., 2014).

Clinical efforts have focused on preventive strategies, with the aim of delaying and ultimately preventing the psychosis onset (Sommer and Arango, 2017; Sommer et al., 2016). UHR individuals have a 15–30% risk of developing full psychotic disorder within 12 months of the first clinical presentation and *a* >36% risk after 3 years (Yung, 2017). Early interventions in this prodromal period before FEP onset, which is characterized by non-specific psychiatric symptoms, have become a major focus of research on schizophrenia (Cannon et al., 2016; Carpenter and Schiffman, 2015; Millan et al., 2016; Sommer and Arango, 2017). On the preclinical side, recent studies have demonstrated that antipsychotics can immediately normalize endogenous antioxidant/anti-inflammatory activity in rat models of neuroinflammation (MacDowell et al., 2013) and stress (MacDowell et al., 2016, 2017c). Additionally, structural brain changes have been prevented or diminished in the MIS model using antipsychotics such as clozapine (Piontkewitz et al., 2009) or risperidone (Piontkewitz et al., 2011) during adolescence.

This study was designed to prevent the brain deficits associated with the MIS model by administration of risperidone, an antipsychotic with anti-inflammatory properties, at an early stage before the onset of disease. To our knowledge, this is the first study to evaluate brain glucose metabolism and morphology using positron emission tomography (PET) with 2-deoxy-2-[^{18}F]fluoro-D-glucose (FDG) and voxel-based morphometry (VBM) approaches adapted to rodents. We also measured the reduction in inflammation and oxidative stress and investigated the improvement in volumetric and metabolic brain changes as outcomes.

2. Experimental procedures

2.1. Animals

Fifty-one Wistar rats were maintained at constant temperature (24 ± 0.5 °C) under 12-h light/dark cycle, with free access to commercial rodent laboratory chow and water. All procedures were conducted in conformity with the European Communities Council Directive 2010/63/EU and approved by the Ethics Committee for Animal Experimentation of our hospital (number ES280790000087). Fig. 1 shows the design of the study.

2.2. Drug treatment

Prenatal Poly I:C was administered as previously described (Hadar et al., 2015). On post-natal day (PND) 21, male offspring were weaned and housed 2–4 per cage.

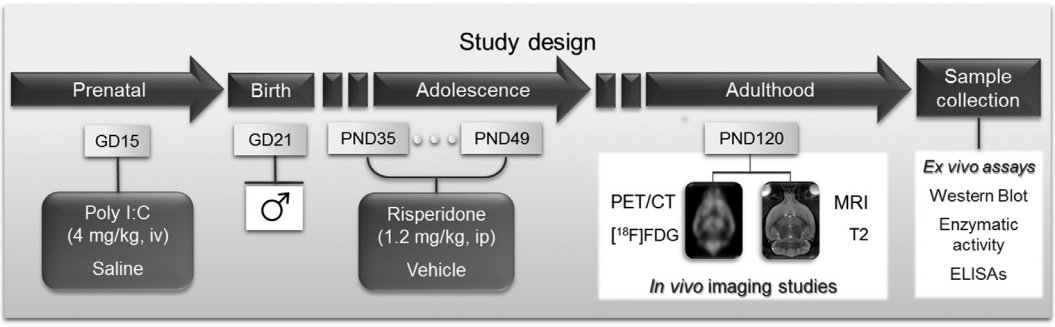

Fig. 1 Study design. Representative diagram of the chronology of the experimental procedures performed during the study according to the age of the animals. Abbrev.: GD, Gestational day; ip, Intraperitoneal; iv, Intravenous; PND, Post-natal day.

Postnatal risperidone was given on PNDs 35–49 (peri-adolescence). Animals received a daily i.p. injection of risperidone (RISP) (1.2 mg/kg) or saline (vehicle). Risperidone (Janssen-Cilag, Spain) was dissolved in 0.1 M tartaric acid (7.5 μL/1 mg) and diluted with saline.

2.3. Imaging studies

Animals were scanned at PND120 (adulthood) (10–15 animals/group).

2.3.1. Magnetic resonance imaging (MRI)

Animals were scanned using a 7-Tesla Biospec 70/20 scanner (Bruker, Germany) under sevoflurane anesthesia (4.5% induction, 2.5% maintenance in 100% O_2). A coronal T2-weighted spin echo sequence was acquired with TE = 33 ms, TR = 3732 ms, averages 2 and slice thickness 0.8 mm (34 slices). Matrix size was 256 × 256 pixels at a FOV of 3.5 × 3.5 cm^2.

2.3.2. Positron emission tomography (PET)

Animals were scanned using a small-animal ARGUS PET/CT scanner (SEDECAL, Spain). Acquisition protocol and reconstruction of the data were performed as previously described (Casquero-Veiga et al., 2018a, b).

2.3.3. Computed tomography (CT)

Studies were acquired using the above-mentioned scanner with the following parameters: 340 mA, 40KV, 360 projections, 8 shots and 200 μm of resolution. Images were reconstructed using a Feldkamp algorithm (isotropic voxel size of 0.121 mm) (Abella et al., 2012).

2.4. Western blot

Frozen tissue samples from the prefrontal cortex (PFC), hippocampus, caudate-putamen, and amygdala of 8–15 animals/group were used for the study of oxidative/nitrosative and inflammatory inducible enzymes such as iNOS and COX-2, as well as the anti-inflammatory regulator inhibitory alpha subunit of nuclear factor kappa-b (IκBα) in cytosolic extracts. Moreover, those brain areas with changes in metabolic activity in the PET studies [retrosplenial cortex (RSA), hypothalamus, ventral and dorsal hippocampus (v/dHipp)] were chosen in 5 animals/group for the study of the neurotrophin BDNF, its main functional full-length tyrosine kinase B receptor (TrkB) and the ionized calcium binding adaptor molecule 1 (iba1). Tissue was solubilized in a 50-mM Tris-hydrochloride (pH 7.7) buffer containing protease and phosphatase inhibitor cocktails (P2714, P5726; Sigma, Spain). Protein levels were measured using the Bradford method.

Expression levels of TrkB, BDNF and iba1 were determined using 50 μg of total protein and 15 μg of cytosolic extract for iNOS, COX2, and IκBα. Proteins were loaded into an electrophoresis gel and blotted onto a membrane with a semi-dry transfer system. Blots were blocked with 5% BSA (Sigma, Spain) and incubated overnight at 4 °C with the following antibodies: rabbit anti-TrkB (sc-12, 1:500), rabbit anti-BDNF (sc-20981, 1:500), rabbit anti-IκBα, (sc-371, 1:1000), rabbit anti-iNOS (sc-650, 1:750), goat anti-COX2 (sc-1747, 1:1000) (SCBT, USA), rabbit anti-iba1 (WEG2172, 1:500; Dako, USA), and rabbit anti-β-actin (A2103, 1:10,000; Sigma, Spain). These primary antibodies were detected using IRDye 800CW goat anti-rabbit secondary antibody (1:10000; LI-COR®, USA) or horseradish peroxidase-linked secondary antibodies. Antibody binding was detected using an Odyssey Fc System (LI-COR®, Germany). All blots were performed at least 3 times in separate assays.

2.5. Nuclear factor kappa B (NFκB) activity

NFκB activation was measured in nuclear extracts (MacDowell et al., 2016) of tissue sample from the PFC, hippocampus, caudate-putamen and amygdala using a commercially ELISA-based system (Cayman Chemical, Estonia).

2.6. Antioxidant enzyme activity

Tissue samples from PFC, hippocampus, caudate-putamen and amygdala were homogenized by sonication in 400 μL PBS (pH7) mixed with a protease inhibitor cocktail (Complete®; Roche), followed by centrifugation at 10,000*g* for 15 min at 4 °C. Supernatants were used for determinations of superoxide dismutase (SOD), catalase (CAT) (Arbor Assay, USA) and glutathione peroxidase (GPx, Cayman Chemical, Estonia). Results were expressed as U/mg of protein.

2.7. Data analysis

Two factors were studied: MIS-model (saline/Poly I:C) and treatment (vehicle/risperidone).

2.7.1. MRI analysis

First, predefined regions of interest (ROIs) of mainly subcortical brain areas were analyzed. Then, a second analysis was performed throughout the entire brain using a VBM approach.

Five manual ROIs were segmented (coordinates from Bregma) (Paxinos and Watson, 2008), as follows: hippocampus (−2.12 to −6.7 mm), lateral ventricles (1.60 to −8.30 mm), caudate-putamen

(1.70 to −1.80 mm), pituitary gland (−4.8 to −6.8 mm) and whole brain. Data were analyzed by means of 2-way ANOVA followed by a pairwise interaction contrast.

MRI processing for VBM was performed by combining different tools (Advanced Normalization Tools [ANTs], Statistical Parametric Mapping software - http://www.fil.ion.ucl.ac.uk/spm/software/spm12 - [SPM12] and ad-hoc scripts developed in Matlab). First, each image was corrected using the N4 bias field correction algorithm (Tustison et al., 2010) and resized by a factor of 10 (Biedermann et al., 2012). These images were linearly realigned to the template image created by Valdes-Hernandez for rat brain (Valdes-Hernandez et al., 2011) and resliced to the template space (isotropic voxel of 1.25 mm) using SPM tools. Second, these data were used to create a rat-specific template by using the ANTs template construction script with the previous Wistar rat brain template (Valdes-Hernandez et al., 2011). This new template was realigned to the Valdesś template image as a starting point. Then, all resliced images were spatially normalized to the custom template using optimized ANTs registration tools. Once all images were in the Wistar rat template space, they were segmented into gray matter (GM), white matter, and cerebrospinal fluid with the SPM *new segment tool* using the probabilistic maps of the Wistar rat brain as priors (Valdes-Hernandez et al., 2011). Afterwards, only GM images were modulated using the Jacobian determinants from the spatial normalization process to preserve gray matter volume within each voxel. Finally, all modulated data were smoothed with a 10-mm FWHM Gaussian kernel. Fig. 2 shows the flow diagram of the structural image processing. The statistical analysis was performed using SPM12 software and groups were compared using an ANOVA test ($p < 0.005$, uncorrected). A 1000-voxel clustering (spatial-extent) threshold was applied to reduce type I error. The statistical analysis with a threshold of $p < 0.01$, uncorrected, is available at the supplementary data (suppl.fig. 1).

2.7.2. PET analysis

PET image post-processing and intensity normalization were performed following protocols previously described (Gasull-Camós et al., 2017). As in the MRI study, PET data was analyzed by predefined ROIs, and a second analysis throughout the entire brain was performed using SPM software.

Six ROIs (whole brain, caudate-putamen, hippocampus, cerebellum, amygdala and temporal cortex) were manually segmented in the MRI template according to the brain atlas (Paxinos and Watson, 2008) in order to determine the intragroup global metabolic differences and corroborate regional SPM results. Data were analyzed using 2-way ANOVA followed by a pairwise interaction contrast.

The voxel-based study was performed by using SPM12 software and groups were compared using an ANOVA test ($p < 0.01$, uncorrected). Since statistics were not corrected for multiple comparisons, the results should be taken with caution because of the unneglectable chance for alpha-errors. A 50-voxel clustering (spatial-extent) threshold was applied to reduce type I error. The statistical analysis with a $p < 0.05$ threshold, uncorrected, is available at the supplementary data (suppl.fig. 2).

2.7.3. Western blot and activity analysis

Western blot digital images were analyzed using densitometry (ImageJ, NIH, USA). Values were normalized to the loading control (β-actin) and expressed as a percent variation from the control. Data from the activity assays were normalized with the protein content of each sample. Data were analyzed by means of 2-way ANOVA followed a by pairwise interaction contrast.

Statistical analysis for ROIs, western blot and enzymatic activity were performed by using IBM SPSS20 and were two-tailed with a p-value of 0.05.

3. Results

3.1. Brain volumetry

Animals weight was analyzed to discard any influence on brain size. ANOVA showed no difference on weight for MIS ($F(1,47) = 2.021$, $p = 0.162$) or treatment ($F(1,47) = 2.081$, $p = 0.156$). No interaction was found ($F(1,47) = 0.008$, $p = 0.929$). Thus, data were not normalized by weight for avoiding to lose any volumetric effect.

3.1.1. *ROI analysis* (Fig. 3B, Suppl, Table 1)

ANOVA revealed a significant effect of MIS in the hippocampus, ventricles and pituitary; with reduced volume in the hippocampus and increased volume in the ventricles, PFC and pituitary in MIS-offspring compared with saline-offspring. Also, a significant effect of risperidone was found in the whole brain, hippocampus and ventricles; with reduced volume in the previous three regions in MIS-offspring. An interaction was found in the caudate-putamen and pituitary.

3.1.2. *VBM analysis* (Fig. 3, Table 1)

3.1.2.1. Pharmacological effect of risperidone. In saline-offspring (Fig. 3A.1, left), risperidone significantly reduced GM volume in the cortex, RSA, vHipp, cerebellar vermis, nucleus accumbens (NAcc), and amygdala-ventral pallidum (VP) and a significant increase in the left entorhinal cortex. In MIS-offspring (Fig. 3A.1, right), risperidone induced lower volume in the cortex, RSA, vHipp, cerebellar vermis, NAcc, amygdala-VP, and the parabrachial nuclei; and higher volume in the prelimbic cortex, caudate-putamen, septum and habenula.

3.1.2.2. Model comparison after each treatment. Vehicle treatment induced significant GM volume reductions in the caudate-putamen, septum, vHipp, RSA, and somatosensory cortex in the MIS-offspring compared to saline-offspring (Fig. 3A.2, left). These changes were greater after risperidone treatment, with significant GM volume reductions in the RSA, cortex, hippocampus, vermis, right VP, amygdala area, caudate-putamen, and cerebellum in MIS-offspring compared with saline-offspring (Fig 3A.2. right).

3.1.2.3. Interaction. An interaction was found in the septo-hippocampal area (Table 1, suppl. Fig. 3).

3.2. Brain metabolism

3.2.1. *ROI analysis* (Fig. 4B., Suppl. Table 1)

ANOVA revealed a significant effect of MIS in the temporal cortex and almost significant in the PFC with reduced metabolism in the hippocampus and increased metabolism in the amygdala in MIS-offspring compared with saline-offspring. A significant effect of risperidone was found in the whole brain, hippocampus, PFC, caudate-putamen, cerebellum and amygdala; with reduced metabolism in the whole brain and cerebellum and increased metabolism in the hippocampus and almost significant in the caudate-putamen. Moreover, an interaction was found in the hippocampus and amygdala.

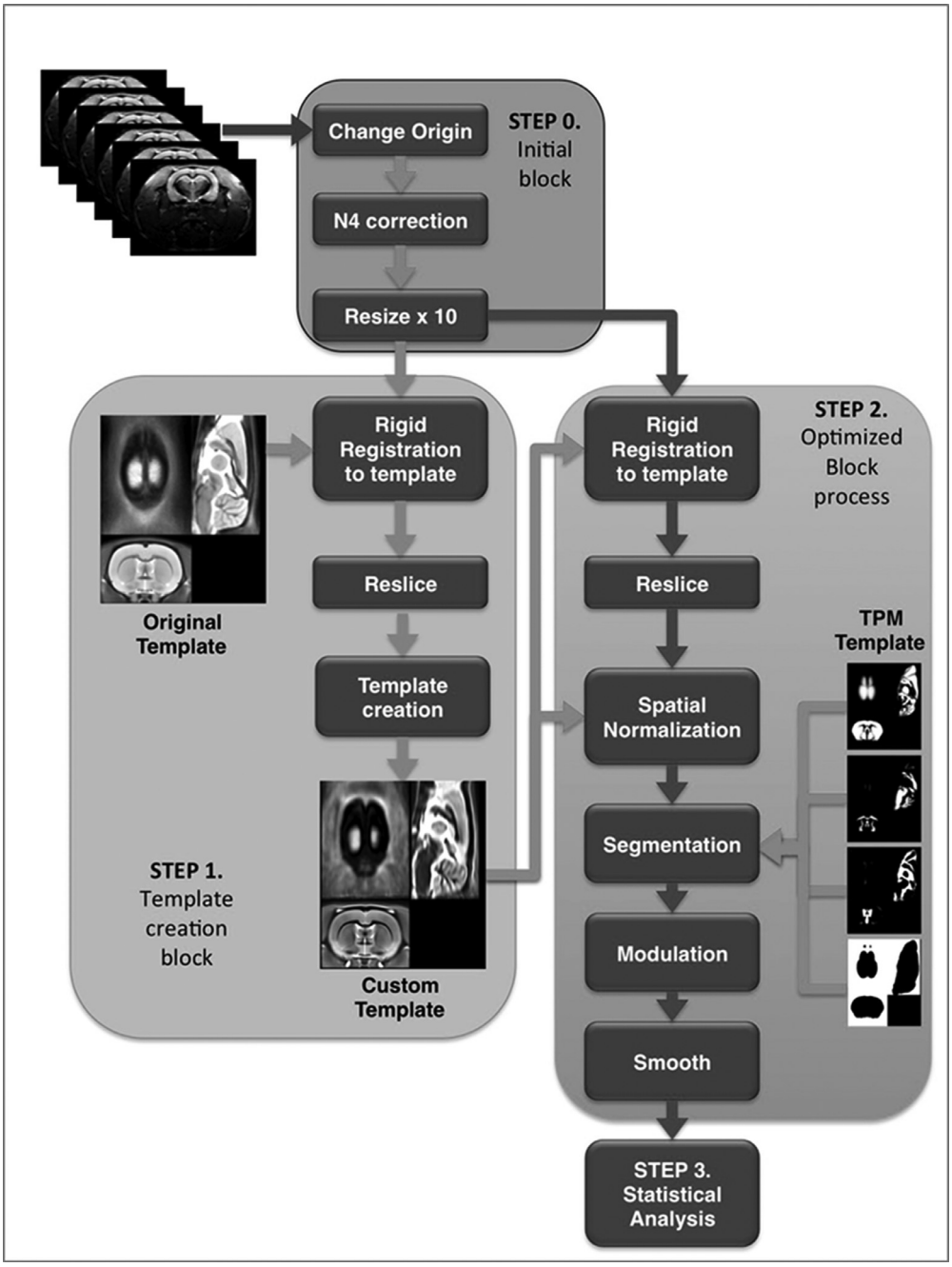

Fig. 2 MRI pipeline for VBM analysis. Schematic flowchart of the MRI processing steps for voxel based morphometry analysis.

3.2.2. SPM analysis

3.2.2.1. Pharmacological effect of risperidone. In saline-offspring (Fig. 4A.1, left), risperidone induced lower glucose metabolism in the olfactory bulb, paraventricular nucleus, cerebellum, septum, hypothalamus, periaqueductal gray matter (PAG), substantia nigra, ventral tegmental area (VTA), and raphe nucleus; and higher uptake in the cingulate cortex, PFC, vHipp, entorhinal cortex and amygdala. In MIS-offspring (Fig. 4A.1, right), risperidone induced lower metabolism in the OB, cerebellum, cortex, medial thalamus, PAG, and VTA and higher uptake in the CC, PFC, vHipp, and brainstem.

3.2.2.2. Model comparison after each treatment. Vehicle-treatment induced lower cortical metabolism and higher metabolism in the NAcc, amygdala and entorhinal cortex in MIS-offspring compared with saline-offspring (Fig. 4A.2, left). Risperidone induced lower metabolism in the cerebellum, PAG, and the parietal cortex and higher FDG uptake in the cingulate cortex, hippocampus-thalamus, and brainstem in MIS-offspring compared with saline-offspring (Fig. 4A.2, right).

3.2.2.3. Interaction. An interaction was found in the brainstem, hippocampus and amygdala-entorhinal cortex (Table 1, suppl. Fig. 3).

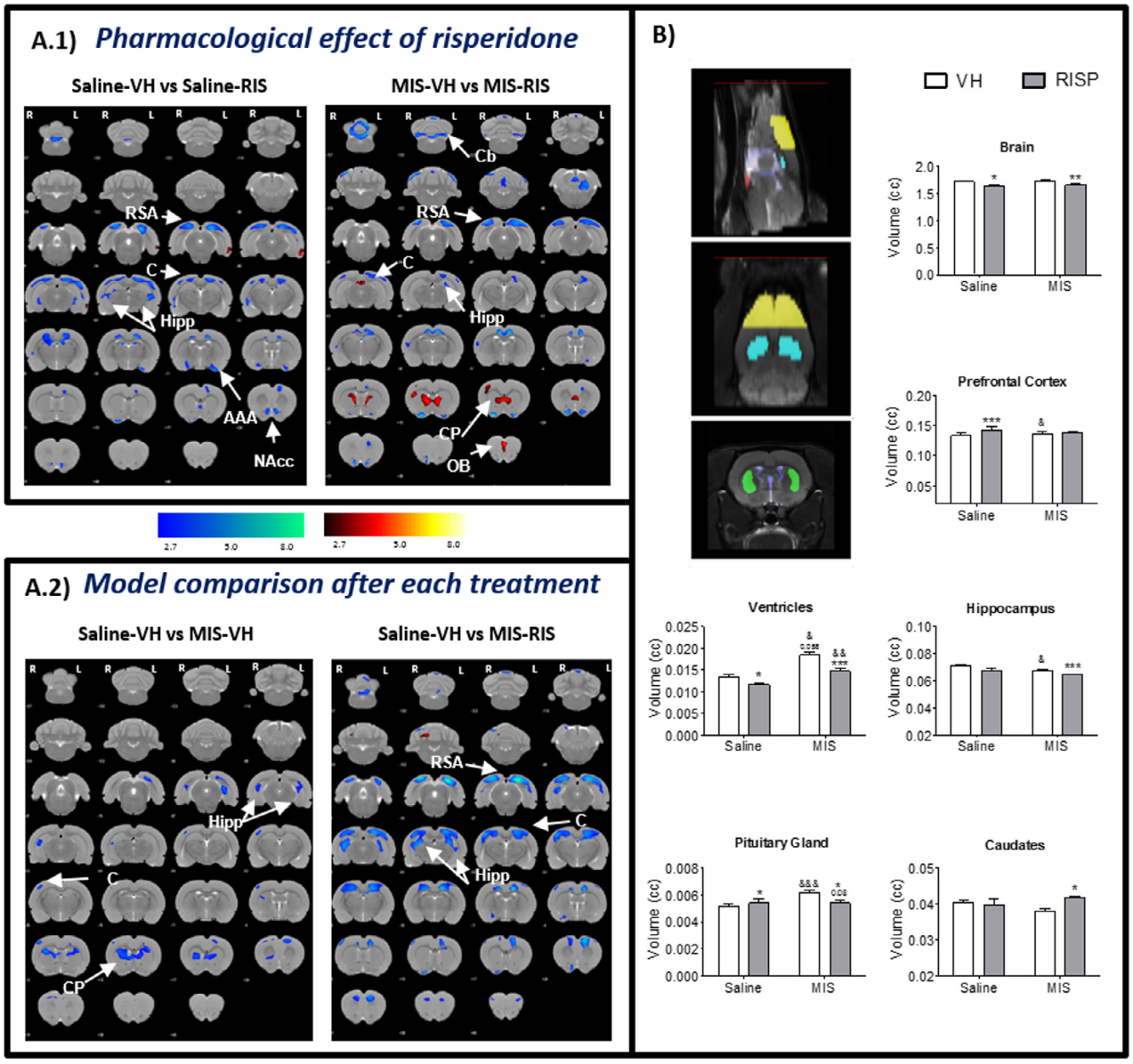

Fig. 3 Volumetric changes measured via MRI. (A) VBM analysis: Colored VBM overlays on the MR reference indicate volume increases (hot colors) or decreases (cold colors). Pharmacological effect of risperidone in saline and MIS-offspring (A.1) and treatment response in MIS animals compared with saline-offspring (A.2). Statistical threshold at $p < 0.005$, uncorrected. The color bars represent the T values corresponding to lower (blue color) and higher (red color) volume. Left (L), Right (R). (AAA: amygdala area, C: cortex, Cb: cerebellum, CP: caudate-putamen, Hipp: hippocampus, NAcc: nucleus accumbens, RSA: retrosplenial cortex, OB: olfactory bulb). (B) ROI analysis: Sagittal, coronal, and axial views of a T2-weighted MR scan of a rat brain. Manual ROIs were placed by identifying the 3D coordinates of each structure on the rat brain atlas (Paxinos and Watson, 2008) and locating the corresponding position in each MRI (red = pituitary; green = caudate; purple = ventricles; blue = hippocampus; and yellow = prefrontal cortex). Global and regional volumetric changes in adulthood after risperidone treatment during adolescence in saline and MIS-offspring. Each column represents the mean ± SEM of 9-14 animals (Saline-VH 11, Saline-RIS 9, MIS-VH 14, MIS-RIS 14). 2-way ANOVA followed by a pairwise interaction contrast [$^{***}p < 0.001$, $^{**}p < 0.01$, $^{*}p < 0.05$ vs vehicle-treated animals, $^{\&\&\&}p < 0.001$, $^{\&\&}p < 0.01$, $^{\&}p < 0.05$ vs saline animals]. (For interpretation of the references to color in this figure legend, the reader is referred to the web version of this article.)

3.3. Neurotrophins

Table 2 and Fig. 5 show the results corresponding to neurotrophins and oxidative/inflammatory parameters.

3.3.1. TrkB

ANOVA revealed a significant effect of MIS in RSA, hypothalamus, ventral and dorsal hippocampus; with a significant reduction in TrkB expression in MIS-offspring compared with saline-offspring. Risperidone did not alter TrkB expression in any area assessed. No interaction was found.

3.3.2. BDNF

ANOVA indicated a significant effect of MIS in RSA. Risperidone did not alter BDNF expression in any area assessed. No interaction was found.

Table 1 Brain volumetric and metabolic changes in the voxel-based analysis.

			A) VOLUMETRIC CHANGES							B) METABOLIC CHANGES						
			ROI	Side	t-value	p_{unc} peak	p_{FDR} peak	p_{FDR} cluster	K	ROI	Side	t-value	p_{unc} peak	p_{FDR} peak	p_{FDR} cluster	K
1. Pharmacological effect of Risperidone	Saline	↓	C-RSA	R	5.10	<0.001	0.099	<0.001	12270	OB		7.09	<0.001	<0.001	<0.001	4783
			C-RSA- vHipp	L	6.34		0.020	<0.001	19576	PVN-Cb-VTA-RN-PAG-hTh-SN-AA		6.52		<0.001		
			vHipp	R	3.93		0.358	0.059	3199							
			Vermis		5.10		0.099	0.165	2066							
			AA	L	4.37		0.274	0.189	1808							
			Nacc-VP		4.73		0.219	0.026	4337							
		↑	Ent C	L	4.80	0.001	0.215	0.393	1680	PFC-Septum-CC		6.86		<0.001		
										vHipp	L	5.30	<0.001	0.001	0.002	3652
											R	3.67		0.061		
	MIS	↓	VP- NAcc	R	7.93	<0.001	<0.001	0.063	3051	OB		6.43	<0.001	<0.001	0.002	4574
				L	5.27		0.019	0.098	2474							
			C-RSA	R	5.58		0.011	0.050	3787	Cb-C-VTA-Th		7.73	<0.001	<0.001		
			C-RSA-vHipp	L	6.38		0.005	<0.001	17894							
			vHipp	R	4.61		0.058	0.403	986							
			Vermis-Cb		6.09		0.003	<0.001	10041							
			PBN		4.64		0.056	0.054	3413							
		↑	PL		5.73	<0.001	0.043	0.114	3043	vHipp-PFC-Septum		8.49	<0.001	<0.001	0.002	4021
			CPu-septum	R	5.01		0.072	0.002	8613							
				L	4.70											
			C	R	4.35		0.088	0.348	1721	CC		6.76		<0.001		
			Habenula		4.54		0.072	0.667	1039	BS		4.44		0.040		
2. Model comparison after each treatment	Vehicle	↓	CPu	R & L	4.56	<0.001	0.497	<0.001	15023	VHipp	R	3.64	<0.001	0.370	0.127	1559
			Septum-SSC	R & L	4.26					C	R & L	3.03	0.002	0.520		
			vHipp-RSA	L	4.18		0.497	0.030	3666	VHipp	L	2.77	0.004	0.596	0.919	64
			vHipp	R	3.62		0.638	0.108	2111							
			SSC	L	4.08		0.497	0.320	1066							
		↑								NAcc-AA-Ent C	L	4.20	<0.001	0.073	0.960	634
											R	3.51	0.001	0.334	0.960	316
										Th	L	2.71	0.005	0.865	0.960	91
	Risperidone	↓	RSA & C-Hipp	L	7.97	<0.001	<0.001	<0.001	66213	OB	R & L	7.25	<0.001	<0.001	0.975	134
				R	6.86		0.001			Cb-C-PAG	R & L	6.04	<0.001	0.001	0.015	3696
			Vermis		4.26	<0.001	0.163	0.060	3749	AA		2.36	0.011	0.967	0.975	89
			VP-AA area	R	5.13		0.052	0.263	2002							
			CPu	R	4.96		0.065	0.527	939							
			Vermis-Cb		4.54		0.092	0.024	4965							
			CSS	R	4.73		0.086	0.527	1198							
		↑								CC-Th	R & L	6.58	<0.001	<0.001	0.003	3390
										vHipp	R & L	6.23		<0.001		
										BS	R & L	4.24		0.066		
Interaction (T value)		↑	Septum		5.40	<0.001	0.052	0.011	5561	BS	R & L	4.02	<0.001	0.258	0.008	1021
										Hipp	R	3.44	0.001	0.291		
		↓								AA-Ent C	L	3.05	0.002	0.953	0.311	177

Effect of risperidone in saline and MIS-offspring (1) and treatment response in MIS-offspring compared with saline-offspring (2). (A) Volumetric changes measured using MRI and (B) Metabolic changes measured using PET.

Type of change (↑ increase, ↓ decrease), ROI: region of interest, Side (L: left, R: right), *t*-value (T), statistical *p*-value (p) (uncorrected and corrected for multiple comparisons, FDR) at peak and cluster level, k (cluster size in number of voxels).

Abbrev.: AA: Amygdala; BS: Brainstem; C: Cortex; Cb: Cerebellum; CC: Cingulate C; CPU: Caudate-putamen; Ent C: Entorhinal C; hTh: Hypothalamus; NAcc: Nucleus accumbens; OB: Olfactory area; PAG: Periaqueductal gray matter; PBN: Parabrachial nucleus; PFC: Prefrontal C; PrL: Prelimbic C; RN: Raphe nucleus; RSA: Retrosplenial C; SN: Substantia nigra; SSC: Somatosensorial C; Th: Thalamus; vHipp: ventral hippocampus; dHipp: Dorsal hippocampus; VP: Ventral pallidum; VTA: Ventral tegmental area.

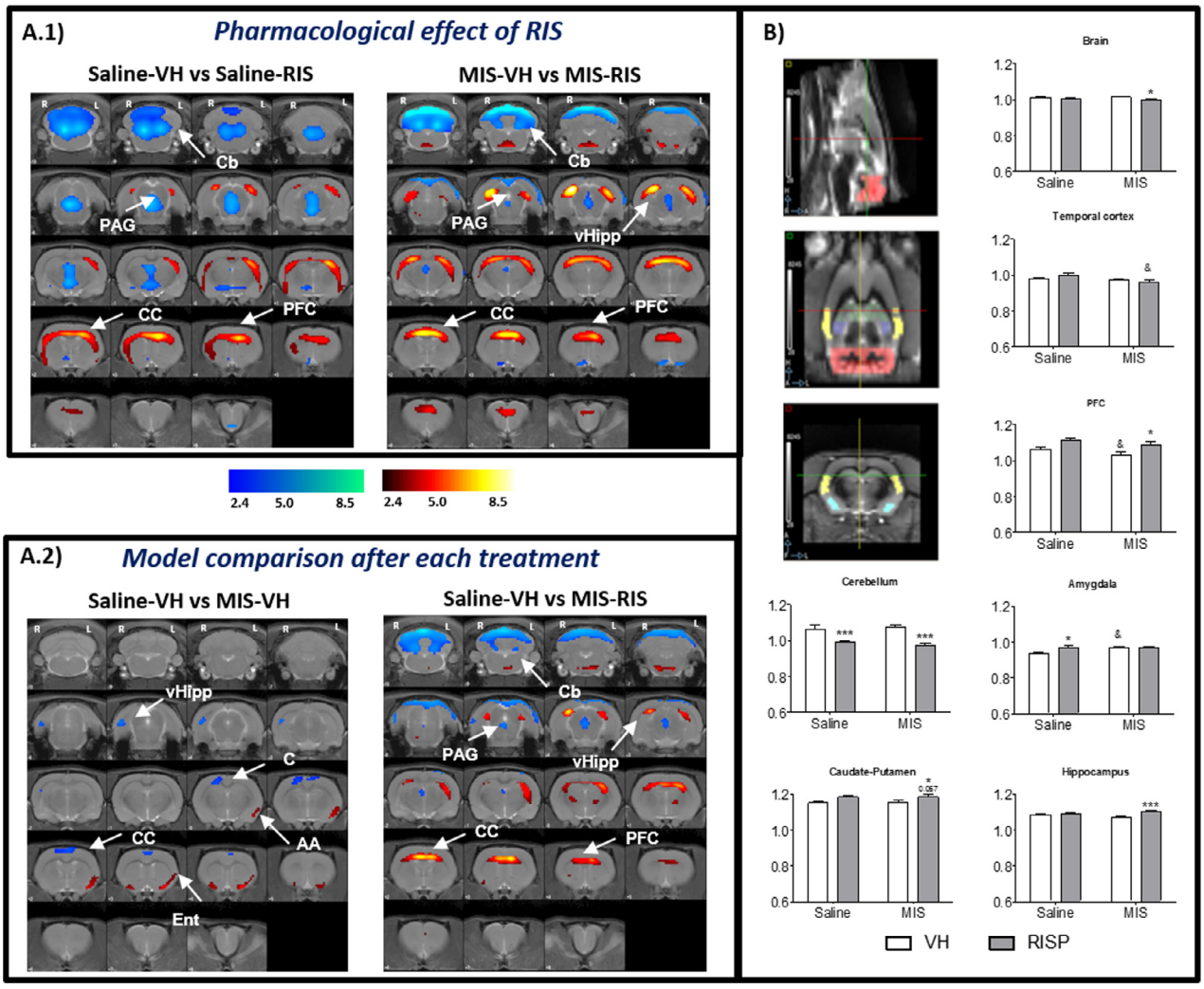

Fig. 4 Brain metabolic changes measured via PET. (A) SPM analysis: Colored PET overlays on the MR reference indicate increased FDG uptake (hot colors) or decreased FDG uptake (cold colors). Pharmacological effect of risperidone in saline and MIS-offspring (A.1) and treatment response in MIS animals compared with saline-offspring (A.2). Statistical threshold at $p < 0.01$, uncorrected. The color bars represent the T values corresponding to lower (blue color) and higher (red color) volume. Left (L), Right (R). (AA-Ent: amygdala-entorhinal area, BS: brainstem, C: cortex, Cb: cerebellum, CC: cingulate cortex, PAG: periaqueductal gray matter, vHipp: ventral hippocampus). (B) ROI analysis: Sagittal, coronal, and axial views of a T1-weighted MR scan of a rat brain. Manual ROIs were placed by identifying the 3D coordinates of each structure on the rat brain atlas (Paxinos and Watson, 2008) and locating the corresponding position in the MRI (red = cerebellum; green = dorsal hippocampus; purple = ventral hippocampus; blue = amygdala; and yellow = temporal cortex). Graphs show the global and regional metabolic changes at adulthood after risperidone treatment during adolescence. Each column represents the mean±SEM of 10–15 animals (Saline-VH 10, Saline-RIS 11, MIS-VH 15, MIS-RIS 15).. 2-way ANOVA followed by a pairwise multiple comparisons test [$^{***}p < 0.001$, $^{**}p < 0.01$, $^{*}p < 0.05$ vs vehicle-treated animals, $^{\&\&\&}p < 0.001$, $^{\&\&}p < 0.01$, $^{\&}p < 0.05$ vs saline animals]. (For interpretation of the references to color in this figure legend, the reader is referred to the web version of this article.)

3.4. Oxidative/inflammatory parameters

3.4.1. iba1

ANOVA revealed a significant effect of MIS in hypothalamus, ventral and dorsal hippocampus of MIS-offspring compared with saline-offspring. Risperidone did not significantly modify its expression. No interaction was found.

3.4.2. NFκB

No MIS effect was found. A significant risperidone effect appeared in PFC, hippocampus and amygdala, with decreased NFκB expression. No interaction was found.

3.4.3. IκBα

A significant MIS effect was found in the PFC, hippocampus and amygdala, with increased IκBα expression in MIS-offspring compared with saline-offspring. A significant risperidone effect was found in the amygdala, with increased expression in MIS-offspring. An interaction was found in the amygdala.

3.4.4. iNOS

ANOVA showed a significant MIS effect in the PFC, hippocampus, caudate-putamen and almost significant effect in the amygdala, with increased iNOS expression in MIS-offspring

Table 2 Risperidone-related effects on the expression of neurotrophic (A) and IOS (B and C) in saline and MIS-offspring.

	MIS	Treatment	Interaction
A) Neurotrophic markers			
TrkB			
Retrosplenial cortex	$F_{(1,16)} = 6.49$ *	$F_{(1,16)} = 0.06$	$F_{(1,16)} = 0.02$
Hypothalamus	$F_{(1,16)} = 79.04$ ***	$F_{(1,16)} = 1.71$	$F_{(1,16)} = 1.39$
Ventral hippocampus	$F_{(1,16)} = 29.64$ ***	$F_{(1,16)} = 0.07$	$F_{(1,16)} = 0.28$
Dorsal hippocampus	$F_{(1,16)} = 32.77$ ***	$F_{(1,16)} = 0.35$	$F_{(1,16)} = 0.44$
BDNF			
Retrosplenial cortex	$F_{(1,15)} = 4.60$ *	$F_{(1,15)} = 1.10$	$F_{(1,15)} = 0.33$
Hypothalamus	$F_{(1,16)} = 1.87$	$F_{(1,16)} = 1.30$	$F_{(1,16)} = 0.64$
Ventral hippocampus	$F_{(1,16)} = 0.01$	$F_{(1,16)} = 0.21$	$F_{(1,16)} = 3.23$
Dorsal hippocampus	$F_{(1,16)} = 1.64$	$F_{(1,16)} = 0.11$	$F_{(1,16)} = 0.64$
B) Inflammatory markers			
iba1			
Retrosplenial cortex	$F_{(1,14)} = 0.03$	$F_{(1,14)} = 0.02$	$F_{(1,14)} = 0.024$
Hypothalamus	$F_{(1,16)} = 13.06$ **	$F_{(1,16)} = 0.02$	$F_{(1,16)} = 1.32$
Ventral hippocampus	$F_{(1,20)} = 1.36$	$F_{(1,20)} = 1.65$	$F_{(1,20)} = 0.07$
Dorsal hippocampus	$F_{(1,20)} = 0.23$	$F_{(1,20)} = 1.22$	$F_{(1,20)} = 0.14$
NFκB			
Prefrontal cortex	$F_{(1,42)} = 1.95$	$F_{(1,42)} = 12.12$**	$F_{(1,42)} = 0.51$
Hippocampus	$F_{(1,42)} = 2.55$	$F_{(1,42)} = 13.36$***	$F_{(1,42)} = 0.74$
Caudate-putamen	$F_{(1,42)} = 0.39$	$F_{(1,42)} = 0.72$	$F_{(1,42)} = 3.49$ * 0.07
Amygdala	$F_{(1,42)} = 1.25$	$F_{(1,42)} = 9.32$ **	$F_{(1,42)} = 0.95$
IκBα			
Prefrontal cortex	$F_{(1,15)} = 8.26$ **	$F_{(1,15)} = 0.27$	$F_{(1,15)} = 0.19$
Hippocampus	$F_{(1,42)} = 6.63$ *	$F_{(1,42)} = 0.62$	$F_{(1,42)} = 1.91$
Caudate-putamen	$F_{(1,42)} = 2.25$	$F_{(1,42)} = 1.41$	$F_{(1,42)} = 1.99$
Amygdala	$F_{(1,42)} = 5.73$ *	$F_{(1,42)} = 6.81$ **	$F_{(1,42)} = 12.27$ ***
iNOS			
Prefrontal cortex	$F_{(1,14)} = 21.58$ ***	$F_{(1,14)} = 1.58$	$F_{(1,14)} = 0.30$
Hippocampus	$F_{(1,42)} = 8.30$ **	$F_{(1,42)} = 0.01$	$F_{(1,42)} = 0.04$
Caudate-putamen	$F_{(1,42)} = 13.83$ ***	$F_{(1,42)} = 3.02$ * 0.09	$F_{(1,42)} = 1.22$
Amygdala	$F_{(1,42)} = 3.01$ 0.09	$F_{(1,42)} = 1.25$	$F_{(1,42)} = 2.22$
COX2			
Prefrontal cortex	$F_{(1,42)} = 2.17$	$F_{(1,42)} = 0.02$	$F_{(1,42)} = 0.06$
Hippocampus	$F_{(1,42)} = 11.17$ **	$F_{(1,42)} = 0.98$	$F_{(1,42)} = 4.07$ *
Caudate-putamen	$F_{(1,42)} = 7.49$ **	$F_{(1,42)} = 1.71$	$F_{(1,42)} = 0.15$
Amygdala	$F_{(1,42)} = 9.78$ *	$F_{(1,42)} = 3.91$ *	$F_{(1,42)} = 2.90$ 0.09
C) Oxidative markers			
CAT			
Prefrontal cortex	$F_{(1,42)} = 2.91$ 0.09	$F_{(1,42)} = 0.48$	$F_{(1,42)} = 2.81$
Hippocampus	$F_{(1,42)} = 14.63$ ***	$F_{(1,42)} = 5.60$ *	$F_{(1,42)} = 10.94$ **
Caudate-putamen	$F_{(1,42)} = 3.72$ 0.06	$F_{(1,42)} = 5.88$ *	$F_{(1,42)} = 1.03$
Amygdala	$F_{(1,42)} = 2.96$ 0.09	$F_{(1,42)} = 1.32$	$F_{(1,42)} = 1.67$
SOD			
Prefrontal cortex	$F_{(1,15)} = 11.00$ **	$F_{(1,15)} = 7.58$ **	$F_{(1,15)} = 1.35$
Hippocampus	$F_{(1,42)} = 0.09$	$F_{(1,42)} = 0.26$	$F_{(1,42)} = 0.47$
Caudate-putamen	$F_{(1,42)} = 1.05$	$F_{(1,42)} = 0.11$	$F_{(1,42)} = 1.19$
Amygdala	$F_{(1,42)} = 3.32$ * 0.08	$F_{(1,42)} = 1.69$	$F_{(1,42)} = 1.04$
GPx			
Prefrontal cortex	$F_{(1,14)} = 12.32$ ***	$F_{(1,14)} = 0.21$	$F_{(1,14)} = 1.78$
Hippocampus	$F_{(1,42)} = 0.96$	$F_{(1,42)} = 0.05$	$F_{(1,42)} = 0.61$
Caudate-putamen	$F_{(1,42)} = 5.71$ *	$F_{(1,42)} = 0.26$	$F_{(1,42)} = 0.20$
Amygdala	$F_{(1,42)} = 0.01$	$F_{(1,42)} = 0.85$	$F_{(1,42)} = 0.29$

Each column represents the ANOVA *F*-test for MIS, risperidone treatment, and its interaction for the studied areas. F: ANOVA *F*-test.
*** $p < 0.001$.
** $p < 0.01$.
* $p < 0.05$.

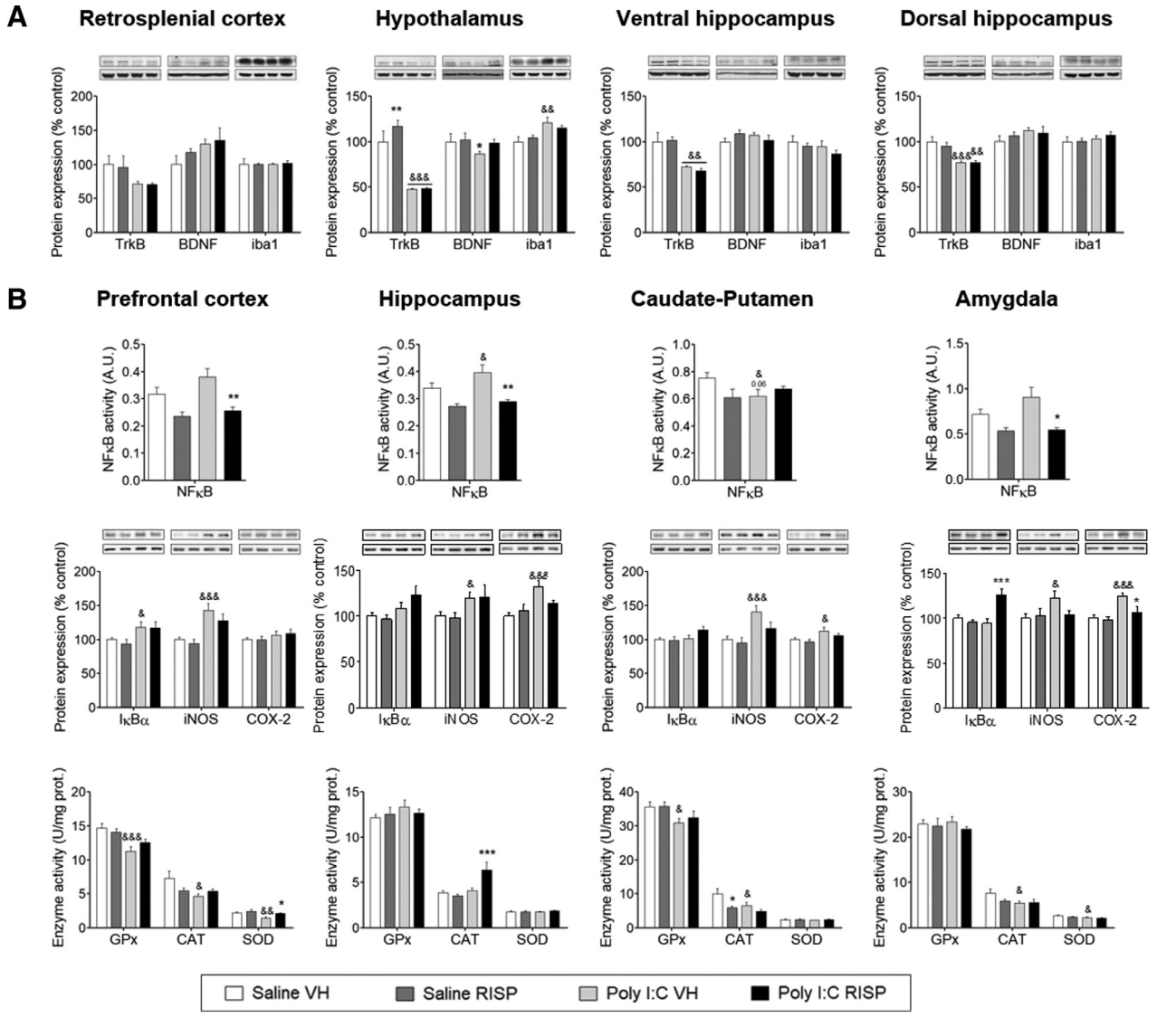

Fig. 5 Risperidone-related effects on the expression of neurotrophic and IOS markers in saline and MIS-offspring. (A) Densitometric analysis of TrkB, BDNF, and iba1 expression in the retrosplenial cortex, hypothalamus, ventral hippocampus, and dorsal hippocampus ($N = 5$–6 animals). Representative bands of TrkB, BDNF, and iba1 (upper bands) and the loading control, β-actin (lower bands), are shown above their corresponding graph bars. (B) NFκB activity, inflammatory marker expression (IκBα, iNOS, COX2), and antioxidant enzyme activity (GPx, CAT, SOD) in the prefrontal cortex, hippocampus, caudate-putamen, and amygdala ($N = 8$–15 animals). Representative bands of IκBα, iNOS, and COX2 (upper bands) and the loading control, β-actin (lower bands), are shown above their corresponding graph bars. Each column represents the mean $\pm$ SEM of 5–8 animals. 2-way ANOVA followed by a pairwise interaction contrast [$^{***}p < 0.001$, $^{**}p < 0.01$, $^{*}p < 0.05$ vs vehicle-treated animals, &&&$p < 0.001$, &&$p < 0.01$, &$p < 0.05$ vs saline animals].

compared with saline-offspring. A nearly significant risperidone effect was found in the caudate-putamen with reduced iNOS expression in MIS-offspring. No interaction was found.

3.4.5. COX2

A significant MIS effect was found in the hippocampus, caudate-putamen and amygdala, with increased COX2 expression in MIS-offspring compared with saline-offspring. A significant risperidone effect was found in the amygdala, with decreased COX2 expression in MIS-offspring. An interaction was found in the hippocampus and almost significant in the amygdala.

3.4.6. GPx

ANOVA revealed a significant MIS effect in the PFC and caudate-putamen, with reduced GPx activity in MIS-offspring compared with saline-offspring. Risperidone did not modify GPx activity. No interaction was found.

3.4.7. CAT

A significant MIS effect was found in the hippocampus and almost significant in the PFC, caudate-putamen and amygdala, with decreased CAT activity in MIS-offspring compared with saline-offspring. A significant risperidone effect was found in the hippocampus and caudate-putamen. An interaction was found in the hippocampus.

3.4.8. SOD

A significant MIS effect was shown in the PFC and almost significant in the amygdala, with lower SOD activity in MIS-offspring compared with saline-offspring. Moreover, a significant risperidone effect was found in the PFC, with increased SOD activity in MIS-offspring. No interaction was found.

4. Discussion

Four are the main findings of this study. Thus, the administration of risperidone during adolescence prevents various schizophrenia-related abnormalities in the MIS model: (1) prevents brain volumetric abnormalities in ventricles and pituitary but decreases the volume in the hippocampus and the total brain, probably due to the risperidone dose used, (2) counteracts cortical and basal ganglia metabolic abnormalities, (3) reduces the expression of brain inflammatory markers but not of OS markers, and (4) does not revert the deficits in the BDNF/TrkB system.

4.1. Risperidone prevents brain volumetric abnormalities in ventricles and pituitary

The many brain volumetric abnormalities associated with schizophrenia and psychosis include reduced volume in global brain and in the frontotemporal cortical and subcortical GM regions and increased volume in ventricles (Haijma et al., 2013; van Erp et al., 2016). UHR subjects also show abnormalities in the PFC and temporal and cingulate cortex before FEP (Chung et al., 2017; de Wit et al., 2016). In this study, we replicated the hallmark of structural abnormalities associated with the MIS model, such as enlarged ventricles and smaller hippocampal volumes (Piontkewitz et al., 2011, 2009). We also observed a reduction in caudate-putamen volume, which has never been reported in the MIS model but has been shown in antipsychotic-naïve FEP patients (Ebdrup et al., 2010).

The effects of risperidone on brain volume in people at UHR of psychosis have received little attention. Only 1 meta-analysis has shown the effects of low-dose risperidone on rates of transition to psychosis, with positive results at 12 months and no difference at 3 years, although the study was subject to several methodological limitations (McGorry et al., 2013). In our study, treatment with risperidone during adolescence prevented enlargement of ventricles in adulthood, as observed by Piontkewitz et al. (2011), although it did not prevent the reduced hippocampal volume in the MIS-offspring reported elsewhere (Piontkewitz et al., 2011, 2009). Failure to see favorable hippocampal changes in MIS compared with saline-offspring could be influenced by the age of the animals scanned compared with Piontkewitz (3-4 months) and by differences in the MRI acquisition protocol and analysis (Piontkewitz et al., 2011). Recent evidences indicate that antipsychotic treatment is associated with changes in hippocampal function and volume that can vary depending on the antipsychotic drug. Thus, aripiprazole, a second-generation antipsychotic (SGA) with partial agonism at 5-HT1A receptors, has been found to increase hippocampal volume in FEPs compared to other SGAs (Bodnar et al., 2016), while quetiapine, a SGA with low agonism at 5-HT1A receptors, have shown loss of hippocampal volume in antipsychotic-naive FEP patients after 6 months of treatment (Ebdrup et al., 2011). At this respect, risperidone a SGA with no agonism at 5-HT1A receptors, would behave as quetiapine, lowering the hippocampal volume. Moreover, we also observed reduced global brain volume in both control and MIS-offspring treated with risperidone. Therefore, volume reduction in this brain area may be related to the high dose used in our study as other authors have pointed out (Massana et al., 2005; Piontkewitz et al., 2011). Of note, we found a positive interaction between MIS and risperidone treatment in the septo-hippocampal area, an area closely connected to the hippocampus, being critical in learning, attention and working memory (Bortz and Grace, 2018). The increased volume of this area in risperidone-treated MIS-offspring could mediate the improvements in prepulse inhibition of acoustic startle (Ma et al., 2004) and latent inhibition (Turgeon et al., 2001) seen in animals with lesions in this area.

Several studies have addressed the effects of risperidone on basal ganglia morphometry, showing increased GM volume in the caudate-putamen after 3 months (Massana et al., 2005) in neuroleptic-naïve FEP patients. Evidence from animal studies showed that haloperidol also induced a significant increase in caudate-putamen volume (Andersson et al., 2002). However, no animal studies have been performed with risperidone. Here, we showed risperidone to be associated with increased caudate-putamen volume in MIS-offspring. It is noteworthy that risperidone was administered over a short period that was critical for neurodevelopment, indicating that the dose of risperidone administered during this window of opportunity must be as low as possible. Therefore, the mechanisms underlying progressive brain changes, such as those due to antipsychotics, warrant further research.

One unexpected result was the increased pituitary volume in MIS-offspring, presumably reflecting activation of the hormonal stress response. Study of the HPA-axis has recently generated considerable interest, since stress has been proposed as a potential trigger of psychosis (Borges et al., 2013; Takahashi et al., 2011). In fact, several studies have shown that FEP patients presented higher levels of plasma cortisol than controls, thus supporting the idea of a hyperactive HPA-axis (Borges et al., 2013; Reniers et al., 2015) which precedes the onset of psychosis (Mondelli, 2014). Specifically, the pituitary is larger in UHR subjects (Nordholm et al., 2013; Pariante, 2008) and, accordingly, our research provides evidence of an activation of the HPA-axis in the MIS model that is supported by reduced hippocampus and increased pituitary volumes. Remarkably, we found that risperidone prevented pituitary enlargement, suggesting that pituitary volume could be considered a new marker of structural abnormalities associated with schizophrenia in the MIS model.

4.2. Risperidone counteracts cortical and basal ganglia metabolic abnormalities

PET studies support the existence of cortical and subcortical dysfunctions (Buchsbaum and Hazlett, 1998; Kim et al., 2017), suggesting that schizophrenia is a disorder with

widespread cerebral dysfunction and neurochemical alterations, including several neurotransmitter systems (Dean, 2012; Frankle et al., 2005; Kim et al., 2015). Specifically, FDG-PET studies in schizophrenia patients have mainly reported decreased glucose metabolism in the whole brain (Volkow et al., 1987), frontal lobe (Bralet et al., 2016; Buchsbaum and Hazlett, 1998), temporal lobe (Bralet et al., 2016; Buchsbaum et al., 2002), parietal lobe (Cleghorn et al., 1989), mediodorsal and centromedial thalamic nuclei (Hazlett et al., 2004), hippocampus (Tamminga et al., 1992), and cingulate cortex (Fujimoto et al., 2007). However, no PET studies have evaluated people at UHR for psychosis (probably due to the radioactive nature of the image study), although efforts are being made to identify neuroimaging indicators of vulnerability to psychosis.

In our study, treatment with risperidone during adolescence prevented the increased metabolism in the nucleus accumbens and the decreased cortical and hippocampal metabolism previously reported by our group in the MIS-offspring compared to saline-offspring (Hadar et al., 2015). Furthermore, a negative interaction is also evident in the amygdala-entorhinal area, showing how risperidone treatment at adolescence induce opposite metabolic responses in healthy and MIS-adult animals. Therefore, this mechanism would suggest a certain counteraction of the increased metabolism in this area in the MIS model (Hadar et al., 2015). Thus, 2 weeks of risperidone treatment during this critical period seem sufficient to alter the profile of limbic metabolism in adulthood, which could probably be responsible for the sensory gating deficits seen in the MIS model (Hadar et al., 2015; Piontkewitz et al., 2011). Remarkably, we found a positive interaction between MIS condition and risperidone treatment in the brainstem and the hippocampus. Both structures are neural targets for risperidone and with well-established roles in cognitive processes (Anwar et al., 2016; Godsil et al., 2013). Thus, this result is consistent with increased perfusion in the brainstem and the posterior hippocampus observed in patients treated with risperidone (Molina et al., 2008).

Moreover, it is noteworthy that risperidone induced decreased metabolism in the cerebellum and PAG in both saline and MIS-offspring. The cerebellum is richly innervated by serotonin, and serotonergic fibers are the third main afferent fibers in the cerebellum (Oostland and van Hooft, 2013). During postnatal cerebellar development, coinciding with the administration of risperidone in this study, serotonin plays a critical role in the stimulation of the growth and formation of dendrites and stabilization of synapses (Oostland and van Hooft, 2013), being responsible for motor and cognitive functions (Bostan et al., 2013; Stoodley et al., 2012). On the other hand, the dopaminergic neurons in the PAG play a key role in the modulation of nociception and the circuits responsible for opiate responding (Eippert and Tracey, 2014; Meyer et al., 2009). Indeed, risperidone proved to induce analgesic effects and enhance the analgesic action of morphine in rats (DiPirro et al., 2011). Consequently, the reduced metabolism shown in the cerebellum and PAG could be related to the effects of risperidone over dopaminergic and serotonergic fibers and could potentially be considered as side effects induced by risperidone. Furthermore, although our approach involved short-term treatment, the dose and frequency used could be associated with the risk of extrapyramidal side effects (Schoretsanitis et al., 2016). However, behavioral studies are needed to corroborate this issue.

4.3. Risperidone reduced expression of brain inflammatory markers but not of OS markers

Our results indicate that the MIS model shows activation of the pro-inflammatory pathway and reduction in the activity of antioxidant enzymes, with marked differences between the brain areas studied. Furthermore, risperidone is able to reduce NFκB activity and iNOS expression in almost all structures at adulthood, except caudate-putamen for NFκB activity and hippocampus for iNOS expression, suggesting that risperidone exerts its anti-inflammatory action mainly through the iNOS pathway.

Adult MIS-offspring exhibited increased expression of intracellular pro-inflammatory molecules in the hippocampus, which could be responsible for the smaller hippocampi found in this study. Microglial activation was also evidenced in the hypothalamus of MIS-offspring and was accompanied by increased iNOS expression. Moreover, we detected higher levels of pro-inflammatory molecules in the caudate-putamen and amygdala, but decreased activity of the antioxidant enzymes CAT and GPx in the PFC and caudate-putamen and of CAT and SOD in the amygdala. The increased microglial activation and iNOS expression, together with the oxidative imbalance, underlay the inflammatory and oxidative etiology of this disorder (Ribeiro et al., 2013). The almost significant trend towards increased NFκB activity in the PFC and hippocampus in the MIS model is noteworthy and may explain the increased expression of its inhibitory subunit IκBα as a compensatory mechanism to restore inflammatory balance, as reported in other experimental settings (MacDowell et al., 2017a). The differences observed between the brain areas studied can be explained by the activation of other products of the antioxidant nuclear factor NRF2 (erythroid 2-related factor 2) pathway, such as HO1 (heme oxygenase-1) and NQO1 (NAD(P)H:quinone oxidoreductase1), and by other counterbalancing mechanisms, such as the anti-inflammatory nuclear factor PPARγ (peroxisome proliferator-activated receptor γ) and the dynamics of microglial activation M1/M2, in which the cytokine environment plays a key role (Martin-Hernandez et al., 2016). Moreover, it was recently reported that *post mortem* brains of chronic schizophrenia patients differently expressed NFκB/IκBα in the PFC and cerebellum, suggesting that the regulation of these elements could differ between these areas (MacDowell et al., 2017b).

Remarkably, we found that risperidone blocks the increase in inflammatory parameters in most of the areas studied, without affecting the OS markers and microglial activation. A large body of evidence indicates that long-term treatment with antipsychotics enhances anti-inflammatory activity and reduces expression of pro-inflammatory markers in patients (Meyer et al., 2011). Nevertheless, no studies have evaluated short-term treatment in young subjects at UHR of psychosis. Preclinical studies have shown that administration of antipsychotics before lipopolysaccharide injection in mice immediately promotes a net anti-inflammatory effect by decreasing

pro-inflammatory cytokine concentrations and enhancing anti-inflammatory cytokine concentrations in serum (Sugino et al., 2009). Moreover, risperidone normalizes elevated levels of inflammatory intracellular mediators and restores the anti-inflammatory pathways mediated by PPARγ in murine neuroinflammation models (MacDowell et al., 2013). In addition, paliperidone, a risperidone metabolite, induces synergic activation and preservation of endogenous antioxidant/anti-inflammatory mechanisms such as the NRF2 and PPARγ pathways in a MIS model administered at low doses for 21 days (MacDowell et al., 2017a).

4.4. Risperidone did not improve MIS-related BDNF/TrkB pathway

We evaluated the expression of BDNF and its receptor TrkB, whose deficits have been linked to various psychiatric disorders (Gupta et al., 2013; Nieto et al., 2013). Our MIS animals exhibited reduced expression of TrkB in the hypothalamus and hippocampus. Moreover, a tendency towards a reduced expression of BDNF was found in the hypothalamus, which would have probably reached statistical significance with a larger sample size. Our results are consistent with previous studies (Barrientos et al., 2003; Gibney et al., 2013), suggesting that the MIS model is associated with an alteration of the BDNF/TrkB system in synaptic plasticity and, consequently, contributes to the pathophysiology in this model. Moreover, the fact that the protein expression abnormalities occurred in the hippocampus and hypothalamus could point to malfunctioning of the HPA-axis in schizophrenia, which would be responsible for the volumetric abnormalities we found in the pituitary and hippocampus of these animals. More studies are necessary to demonstrate this HPA-axis disorder.

The 2-week treatment with risperidone during adolescence seems to improve the reduced BDNF expression tendency in the hypothalamus of adult MIS-offspring. Antipsychotics generally act by blocking dopamine transmission at D2-like receptors; specifically, BDNF controls expression of one of these receptors. Thus, BDNF has been linked to the dopamine neurotransmission pathway in schizophrenia and its treatment (Guillin et al., 2007), with higher plasma BDNF levels indicating a better response to antipsychotics (Lee and Kim, 2009). Our results and these findings reinforce the involvement of the HPA-axis in the MIS model and the hypothalamic tissue-specific site of action of antipsychotics.

4.5. Limitations

Our study is subject to several limitations. The first is the animal model used. Although the MIS model is a well-validated model of schizophrenia, animal models cannot fully reproduce this uniquely human disorder. Nevertheless, they causally demonstrate that early interventions can prevent the emergence of schizophrenia-like phenotypes. Second, we evaluated an antipsychotic with anti-inflammatory properties for prevention of schizophrenia. Risperidone was chosen, since it is widely used in young children with pervasive developmental disorders and autism and in high-risk individuals, and proved effective in a neurodevelopmental animal model (Aman et al., 2015; Piontkewitz et al., 2011; Vitiello et al., 2009). However, additional prevention studies with new agents are necessary.

5. Conclusion

To our knowledge, this is the first PET study to show that treatment with risperidone during adolescence prevents various schizophrenia-related metabolic brain abnormalities at adulthood in the experimental MIS model in rats, such as the hippocampal and cortical metabolism reduction. We also demonstrated dysregulation of inflammatory markers and impairment of the HPA-axis, i.e., higher pituitary volume, which are partially counteracted by the action of risperidone during this critical period in the MIS animal model. In summary, our study suggests that some schizophrenia-related changes in inflammation and oxidative stress can be prevented in the MIS model and highlights the need for novel strategies to alter disease course based on anti-inflammatory compounds in risk populations at early stages.

Declaration of Competing Interest

DF has been a consultant for and/or has received fees from Janssen, Lundbeck, Otsuka, EISAI, and IE4Lab. CA has been a consultant for or has received honoraria or grants from Acadia, Abbot, AMGEN, AstraZeneca, Bristol-Myers Squibb, Caja Navarra, CIBERSAM, Fundación Alicia Koplowitz, Forum, Instituto de Salud Carlos III, Gedeon Richter, Janssen Cilag, Lundbeck, Merck, Ministerio de Ciencia e Innovación, Ministerio de Sanidad, Ministerio de Economía y Competitividad, Mutua Madrileña, Ots uka, Pfizer, Roche, Servier, Shire, Schering Plough, Sumitomo Dainippon Pharma, Sunovio and Takeda. All other authors declare that they have no conflict of interest.

CRediT authorship contribution statement

Marta Casquero-Veiga: Data curation, Writing - original draft, Validation. **David García-García:** Data curation, Validation. **Karina S. MacDowell:** Data curation, Validation. **Laura Pérez-Caballero:** Data curation, Validation. **Sonia Torres-Sánchez:** Data curation, Validation. **David Fraguas:** Writing - review & editing, Validation. **Esther Berrocoso:** Data curation, Validation. **Juan C. Leza:** Data curation, Writing - review & editing, Validation. **Celso Arango:** Writing - review & editing, Validation. **Manuel Desco:** Methodology, Writing - review & editing, Validation. **María Luisa Soto-Montenegro:** Conceptualization, Data curation, Methodology, Writing - review & editing, Validation.

Role of funding source

MLS was supported by the Ministerio de Ciencia, Innovación y Universidades, Instituto de Salud Carlos III, projects PI14/00860, CPII14/00005, MV15/00002 and PI17/01766 cofunded by European Regional Development Fund (ERDF), "A way of making Europe", CIBERSAM, Delegación del Gobierno para el Plan Nacional sobre Drogas (PNSD2017/085)

and Fundación Alicia Koplowitz (FAK16/01). MD was supported by Comunidad de Madrid (BRADE-CM S2013/ICE-2958). MCV was supported by Fundación Tatiana Pérez de Guzmán el Bueno. CA and DF were supported by the Ministerio de Ciencia, Innovación y Universidades, Instituto de Salud Carlos III, co-funded by European Regional Development Fund (ERDF), "A way of making Europe", CIBERSAM, Madrid Regional Government (B2017/BMD-3740 AGES-CM-2), European Union Structural Funds, European Union Seventh Framework Program under grant agreements FP7-HEALTH-2009-2.2.1-2-241909 (Project EU-GEI), FP7-HEALTH-2009-2.2.1-3-242114 (Project OPTiMISE), FP7- HEALTH-2013-2.2.1-2-603196 (Project PSYSCAN), and FP7-HEALTH-2013-2.2.1-2-602478 (Project METSY), and the European Union H2020 Program under the Innovative Medicines Initiative 2 Joint Undertaking (grant agreement No 115916; Project PRISM), Fundación Familia Alonso, Fundación Alicia Koplowitz, Fundación Mutua Madrileña, and ERA-NET NEURON (Network of European Funding for Neuroscience Research). KMcD and JCL were supported by ISCIII FlammPEPS and MINECO SAF16-75500-R. The funding sources did not play any role in the design or writing of the manuscript.

Acknowledgements

We thank Alexandra de Francisco and Yolanda Sierra for their support in animal handling, drug administration, and image acquisition. We thank Ana Romero and Joaquin Redondo for their support in the Western blot analysis.

Supplementary materials

Supplementary material associated with this article can be found, in the online version, at doi:10.1016/j.euroneuro.2019.05.002.

References

Abella, M., Vaquero, J.J., Sisniega, A., Pascau, J., Udías, A., García, V., Vidal, I., Desco, M., 2012. Software architecture for multi-bed FDK-based reconstruction in X-ray CT scanners. Comput. Meth. Prog. Bio. 107, 218–232.

Aman, M., Rettiganti, M., Nagaraja, H.N., Hollway, J.A., McCracken, J., McDougle, C.J., Tierney, E., Scahill, L., Arnold, L.E., Hellings, J., Posey, D.J., Swiezy, N.B., Ghuman, J., Grados, M., Shah, B., Vitiello, B., 2015. Tolerability, safety, and benefits of risperidone in children and adolescents with autism: 21-month follow-up after 8-week placebo-controlled trial. J. Child Adolesc. Psychopharmacol. 25, 482–493.

Andersson, C., Hamer, R.M., Lawler, C.P., Mailman, R.B., Lieberman, J.A., 2002. Striatal volume changes in the rat following long-term administration of typical and atypical antipsychotic drugs. Neuropsychopharmacology 27, 143–151.

Anwar, I.J., Miyata, K., Zsombok, A., 2016. Brain stem as a target site for the metabolic side effects of olanzapine. J. Neurophysiol. 115, 1389–1398.

Barrientos, R.M., Sprunger, D.B., Campeau, S., Higgins, E.A., Watkins, L.R., Rudy, J.W., Maier, S.F., 2003. Brain-derived neurotrophic factor mRNA downregulation produced by social isolation is blocked by intrahippocampal interleukin-1 receptor antagonist. Neuroscience 121, 847–853.

Biedermann, S., Fuss, J., Zheng, L., Sartorius, A., Falfan-Melgoza, C., Demirakca, T., Gass, P., Ende, G., Weber-Fahr, W., 2012. In vivo voxel based morphometry: detection of increased hippocampal volume and decreased glutamate levels in exercising mice. NeuroImage 61, 1206–1212.

Blomstrom, A., Karlsson, H., Gardner, R., Jorgensen, L., Magnusson, C., Dalman, C., 2016. Associations between maternal infection during pregnancy, childhood infections, and the risk of subsequent psychotic disorder–a Swedish cohort study of nearly 2 million individuals. Schizophr. Bull. 42, 125–133.

Bodnar, M., Malla, A.K., Makowski, C., Chakravarty, M.M., Joober, R., Lepage, M., 2016. The effect of second-generation antipsychotics on hippocampal volume in first episode of psychosis: longitudinal study. BJPsych Open 2, 139–146.

Borges, S., Gayer-Anderson, C., Mondelli, V., 2013. A systematic review of the activity of the hypothalamic-pituitary-adrenal axis in first episode psychosis. Psychoneuroendocrinology 38, 603–611.

Bortz, D.M., Grace, A.A., 2018. Medial septum differentially regulates dopamine neuron activity in the rat ventral tegmental area and substantia nigra via distinct pathways. Neuropsychopharmacology 43, 2093–2100.

Bostan, A.C., Dum, R.P., Strick, P.L., 2013. Cerebellar networks with the cerebral cortex and basal ganglia. Trends Cogn. Sci. 17, 241–254.

Bralet, M.C., Buchsbaum, M.S., DeCastro, A., Shihabuddin, L., Mitelman, S.A., 2016. FDG-PET scans in patients with Kraepelinian and non-Kraepelinian schizophrenia. Eur. Arch. Psychiatry Clin. Neurosci. 266, 481–494.

Buchsbaum, M.S., Hazlett, E.A., 1998. Positron emission tomography studies of abnormal glucose metabolism in schizophrenia. Schizophr. Bull. 24, 343–364.

Buchsbaum, M.S., Nenadic, I., Hazlett, E.A., Spiegel-Cohen, J., Fleischman, M.B., Akhavan, A., Silverman, J.M., Siever, L.J., 2002. Differential metabolic rates in prefrontal and temporal Brodmann areas in schizophrenia and schizotypal personality disorder. Schizophr. Res. 54, 141–150.

Cannon, T.D., Yu, C., Addington, J., Bearden, C.E., Cadenhead, K.S., Cornblatt, B.A., Heinssen, R., Jeffries, C.D., Mathalon, D.H., McGlashan, T.H., Perkins, D.O., Seidman, L.J., Tsuang, M.T., Walker, E.F., Woods, S.W., Kattan, M.W., 2016. An individualized risk calculator for research in prodromal psychosis. Am. J. Psychiatry 173, 980–988.

Carpenter, W.T., Schiffman, J., 2015. Diagnostic Concepts in the Context of Clinical High Risk/Attenuated Psychosis Syndrome. Schizophr. Bull. 41, 1001–1002.

Casquero-Veiga, M., Garcia-Garcia, D., Desco, M., Soto-Montenegro, M.L., 2018a. Understanding Deep brain stimulation: in vivo metabolic consequences of the electrode insertional effect. BioMed Res. Int. 2018, 8560232.

Casquero-Veiga, M., Garcia-Garcia, D., Pascau, J., Desco, M., Soto-Montenegro, M.L., 2018b. Stimulating the nucleus accumbens in obesity: a positron emission tomography study after deep brain stimulation in a rodent model. PloS One 13, e0204740.

Cleghorn, J.M., Garnett, E.S., Nahmias, C., Firnau, G., Brown, G.M., Kaplan, R., Szechtman, H., Szechtman, B., 1989. Increased frontal and reduced parietal glucose metabolism in acute untreated schizophrenia. Psychiatry Res. 28, 119–133.

Chung, Y., Haut, K.M., He, G., van Erp, T.G.M., McEwen, S., Addington, J., Bearden, C.E., Cadenhead, K., Cornblatt, B., Mathalon, D.H., McGlashan, T., Perkins, D., Seidman, L.J., Tsuang, M., Walker, E., Woods, S.W., Cannon, T.D.North American Prodrome Longitudinal Study, C., 2017. Ventricular enlargement and progressive reduction of cortical gray matter are linked in prodromal youth who develop psychosis. Schizophr. Res. 189, 169–174.

de Wit, S., Wierenga, L.M., Oranje, B., Ziermans, T.B., Schothorst, P.F., van Engeland, H., Kahn, R.S., Durston, S., 2016. Brain development in adolescents at ultra-high risk for psychosis: longitudinal changes related to resilience. NeuroImage. Clin. 12, 542–549.

Dean, B., 2012. Neurochemistry of schizophrenia: the contribution of neuroimaging postmortem pathology and neurochemistry in schizophrenia. Curr. Top. Med. Chem. 12, 2375–2392.

DiPirro, J.M., Thompson, A.C., Suarez, M., Leo, R.J., 2011. Low doses of risperidone and morphine interact to produce more analgesia and greater extrapyramidal effects in rats. Neurosci. Lett. 490, 21–26.

Ebdrup, B.H., Glenthoj, B., Rasmussen, H., Aggernaes, B., Langkilde, A.R., Paulson, O.B., Lublin, H., Skimminge, A., Baare, W., 2010. Hippocampal and caudate volume reductions in antipsychotic-naive first-episode schizophrenia. J. Psychiatry Neurosci. 35, 95–104.

Ebdrup, B.H., Skimminge, A., Rasmussen, H., Aggernaes, B., Oranje, B., Lublin, H., Baare, W., Glenthoj, B., 2011. Progressive striatal and hippocampal volume loss in initially antipsychotic-naive, first-episode schizophrenia patients treated with quetiapine: relationship to dose and symptoms. Int. J. Neuropsychopharmacol. 14, 69–82.

Eippert, F., Tracey, I., 2014. Pain and the PAG: learning from painful mistakes. Nat. Neurosci. 17, 1438–1439.

Frankle, W.G., Narendran, R., Huang, Y., Hwang, D.R., Lombardo, I., Cangiano, C., Gil, R., Laruelle, M., Abi-Dargham, A., 2005. Serotonin transporter availability in patients with schizophrenia: a positron emission tomography imaging study with [11C]DASB. Biol. Psychiatry 57, 1510–1516.

Fujimoto, T., Takeuch, K., Matsumoto, T., Kamimura, K., Hamada, R., Nakamura, K., Kato, N., 2007. Abnormal glucose metabolism in the anterior cingulate cortex in patients with schizophrenia. Psychiatry Res. 154, 49–58.

Gardner, R.M., Dalman, C., Wicks, S., Lee, B.K., Karlsson, H., 2013. Neonatal levels of acute phase proteins and later risk of non-affective psychosis. Transl. Psychiatry 3, e228.

Gasull-Camós, J., Soto-Montenegro, M.L., Casquero-Veiga, M., Desco, M., Artigas, F., Castañé, A., 2017. Differential patterns of subcortical activity evoked by glial GLT-1 blockade in prelimbic and infralimbic cortex: relationship to antidepressant-like effects in rats. Int. J. Neuropsychopharmacol. (in press).

Gibney, S.M., McGuinness, B., Prendergast, C., Harkin, A., Connor, T.J., 2013. Poly I:c-induced activation of the immune response is accompanied by depression and anxiety-like behaviours, kynurenine pathway activation and reduced BDNF expression. Brain Behav. Immun. 28, 170–181.

Godsil, B.P., Kiss, J.P., Spedding, M., Jay, T.M., 2013. The hippocampal-prefrontal pathway: the weak link in psychiatric disorders? Eur. Neuropsychopharmacol. 23, 1165–1181.

Guillin, O., Demily, C., Thibaut, F., 2007. Brain-derived neurotrophic factor in schizophrenia and its relation with dopamine. Int. Rev. Neurobiol. 78, 377–395.

Gupta, V.K., You, Y., Gupta, V.B., Klistorner, A., Graham, S.L., 2013. TrkB receptor signalling: implications in neurodegenerative, psychiatric and proliferative disorders. Int. J. Mol. Sci. 14, 10122–10142.

Hadar, R., Soto-Montenegro, M.L., Gotz, T., Wieske, F., Sohr, R., Desco, M., Hamani, C., Weiner, I., Pascau, J., Winter, C., 2015. Using a maternal immune stimulation model of schizophrenia to study behavioral and neurobiological alterations over the developmental course. Schizophr. Res. 166, 238–247.

Haijma, S.V., Van Haren, N., Cahn, W., Koolschijn, P.C., Hulshoff Pol, H.E., Kahn, R.S., 2013. Brain volumes in schizophrenia: a meta-analysis in over 18 000 subjects. Schizophr. Bull. 39, 1129–1138.

Hazlett, E.A., Buchsbaum, M.S., Kemether, E., Bloom, R., Platholi, J., Brickman, A.M., Shihabuddin, L., Tang, C., Byne, W., 2004. Abnormal glucose metabolism in the mediodorsal nucleus of the thalamus in schizophrenia. Am. J. Psychiatry 161, 305–314.

Kim, J.H., Kim, J.H., Son, Y.D., Joo, Y.H., Lee, S.Y., Kim, H.K., Woo, M.K., 2017. Altered interregional correlations between serotonin transporter availability and cerebral glucose metabolism in schizophrenia: a high-resolution PET study using [11C]DASB and [18F]FDG. Schizophr. Res. 182, 55–65.

Kim, J.H., Son, Y.D., Kim, J.H., Choi, E.J., Lee, S.Y., Lee, J.E., Cho, Z.H., Kim, Y.B., 2015. Serotonin transporter availability in thalamic subregions in schizophrenia: a study using 7.0-T MRI with [(11)C]DASB high-resolution PET. Psychiatry Res. 231, 50–57.

Lee, B.H., Kim, Y.K., 2009. Increased plasma brain-derived neurotropic factor, not nerve growth factor-Beta, in schizophrenia patients with better response to risperidone treatment. Neuropsychobiology 59, 51–58.

Ma, J., Shen, B., Rajakumar, N., Leung, L.S., 2004. The medial septum mediates impairment of prepulse inhibition of acoustic startle induced by a hippocampal seizure or phencyclidine. Behav. Brain Res. 155, 153–166.

MacDowell, K.S., Caso, J.R., Martin-Hernandez, D., Moreno, B.M., Madrigal, J.L., Mico, J.A., Leza, J.C., Garcia-Bueno, B., 2016. The atypical antipsychotic paliperidone regulates endogenous antioxidant/anti-inflammatory pathways in rat models of acute and chronic restraint stress. Neurotherapeutics 13, 833–843.

MacDowell, K.S., Garcia-Bueno, B., Madrigal, J.L., Parellada, M., Arango, C., Mico, J.A., Leza, J.C., 2013. Risperidone normalizes increased inflammatory parameters and restores anti-inflammatory pathways in a model of neuroinflammation. Int. J. Neuropsychopharmacol. 16, 121–135.

MacDowell, K.S., Munarriz-Cuezva, E., Caso, J.R., Madrigal, J.L., Zabala, A., Meana, J.J., Garcia-Bueno, B., Leza, J.C., 2017a. Paliperidone reverts Toll-like receptor 3 signaling pathway activation and cognitive deficits in a maternal immune activation mouse model of schizophrenia. Neuropharmacology 116, 196–207.

MacDowell, K.S., Pinacho, R., Leza, J.C., Costa, J., Ramos, B., Garcia-Bueno, B., 2017b. Differential regulation of the TLR4 signalling pathway in post-mortem prefrontal cortex and cerebellum in chronic schizophrenia: relationship with SP transcription factors. Prog. Neuro-Psychopharmacol. Biol. Psychiatry 79, 481–492.

MacDowell, K.S., Sayd, A., Garcia-Bueno, B., Caso, J.R., Madrigal, J.L.M., Leza, J.C., 2017c. Effects of the antipsychotic paliperidone on stress-induced changes in the endocannabinoid system in rat prefrontal cortex. World J. Biol. Psychiatry 18, 457–470.

Martin-Hernandez, D., Bris, A.G., MacDowell, K.S., Garcia-Bueno, B., Madrigal, J.L., Leza, J.C., Caso, J.R., 2016. Modulation of the antioxidant nuclear factor (erythroid 2-derived)-like 2 pathway by antidepressants in rats. Neuropharmacology 103, 79–91.

Massana, G., Salgado-Pineda, P., Junque, C., Perez, M., Baeza, I., Pons, A., Massana, J., Navarro, V., Blanch, J., Morer, A., Mercader, J.M., Bernardo, M., 2005. Volume changes in gray matter in first-episode neuroleptic-naive schizophrenic patients treated with risperidone. J. Clin. Psychopharmacol. 25, 111–117.

McGorry, P.D., Nelson, B., Phillips, L.J., Yuen, H.P., Francey, S.M., Thampi, A., Berger, G.E., Amminger, G.P., Simmons, M.B., Kelly, D., Dip, G., Thompson, A.D., Yung, A.R., 2013. Randomized controlled trial of interventions for young people at ultra-high risk of psychosis: twelve-month outcome. J. Clin. Psychiatry 74, 349–356.

Meyer, P.J., Morgan, M.M., Kozell, L.B., Ingram, S.L., 2009. Contribution of dopamine receptors to periaqueductal gray-mediated antinociception. Psychopharmacology 204, 531–540.

Meyer, U., Schwarz, M.J., Muller, N., 2011. Inflammatory processes in schizophrenia: a promising neuroimmunological target for the treatment of negative/cognitive symptoms and beyond. Pharmacol. Therap. 132, 96–110.

Millan, M.J., Andrieux, A., Bartzokis, G., Cadenhead, K., Dazzan, P., Fusar-Poli, P., Gallinat, J., Giedd, J., Grayson, D.R., Heinrichs, M., Kahn, R., Krebs, M.O., Leboyer, M., Lewis, D., Marin, O., Marin, P., Meyer-Lindenberg, A., McGorry, P., McGuire, P., Owen, M.J., Patterson, P., Sawa, A., Spedding, M., Uhlhaas, P., Vaccarino, F., Wahlestedt, C., Weinberger, D., 2016. Altering the course of schizophrenia: progress and perspectives. Nat. Rev. 15, 485–515.

Molina, V., Tamayo, P., Montes, C., De Luxan, A., Martin, C., Rivas, N., Sancho, C., Dominguez-Gil, A., 2008. Clozapine may partially compensate for task-related brain perfusion abnormalities in risperidone-resistant schizophrenia patients. Prog. Neuro-Psychopharmacol. Biol. Psychiatry 32, 948–954.

Mondelli, V., 2014. From stress to psychosis: whom, how, when and why? Epidemiol. Psychiatric Sci. 23, 215–218.

Nieto, R., Kukuljan, M., Silva, H., 2013. BDNF and schizophrenia: from neurodevelopment to neuronal plasticity, learning, and memory. Front. Psychiatry 4, 45.

Nordholm, D., Krogh, J., Mondelli, V., Dazzan, P., Pariante, C., Nordentoft, M., 2013. Pituitary gland volume in patients with schizophrenia, subjects at ultra high-risk of developing psychosis and healthy controls: a systematic review and meta-analysis. Psychoneuroendocrinology 38, 2394–2404.

Oostland, M., van Hooft, J.A., 2013. The role of serotonin in cerebellar development. Neuroscience 248, 201–212.

Pariante, C.M., 2008. Pituitary volume in psychosis: the first review of the evidence. J. Psychopharmacol. 22, 76–81.

Paxinos, G., Watson, C., 2008. The Rat Brain in Stereotaxic Coordinates, fourth ed. Academic Press, San Diego.

Piontkewitz, Y., Arad, M., Weiner, I., 2011. Risperidone administered during asymptomatic period of adolescence prevents the emergence of brain structural pathology and behavioral abnormalities in an animal model of schizophrenia. Schizophr. Bull. 37, 1257–1269.

Piontkewitz, Y., Assaf, Y., Weiner, I., 2009. Clozapine administration in adolescence prevents postpubertal emergence of brain structural pathology in an animal model of schizophrenia. Biol. Psychiatry 66, 1038–1046.

Reniers, R.L., Garner, B., Phassouliotis, C., Phillips, L.J., Markulev, C., Pantelis, C., Bendall, S., McGorry, P.D., Wood, S.J., 2015. The relationship between stress, HPA axis functioning and brain structure in first episode psychosis over the first 12 weeks of treatment. Psychiatry Res. 231, 111–119.

Ribeiro, B.M., do Carmo, M.R., Freire, R.S., Rocha, N.F., Borella, V.C., de Menezes, A.T., Monte, A.S., Gomes, P.X., de Sousa, F.C., Vale, M.L., de Lucena, D.F., Gama, C.S., Macedo, D., 2013. Evidences for a progressive microglial activation and increase in iNOS expression in rats submitted to a neurodevelopmental model of schizophrenia: reversal by clozapine. Schizophr. Res. 151, 12–19.

Ripke, S., O'Dushlaine, C., Chambert, K., Moran, J.L., Kahler, A.K., Akterin, S., Bergen, S.E., Collins, A.L., Crowley, J.J., Fromer, M., Kim, Y., Lee, S.H., Magnusson, P.K., Sanchez, N., Stahl, E.A., Williams, S., Wray, N.R., Xia, K., Bettella, F., Borglum, A.D., Bulik-Sullivan, B.K., Cormican, P., Craddock, N., de Leeuw, C., Durmishi, N., Gill, M., Golimbet, V., Hamshere, M.L., Holmans, P., Hougaard, D.M., Kendler, K.S., Lin, K., Morris, D.W., Mors, O., Mortensen, P.B., Neale, B.M., O'Neill, F.A., Owen, M.J., Milovancevic, M.P., Posthuma, D., Powell, J., Richards, A.L., Riley, B.P., Ruderfer, D., Rujescu, D., Sigurdsson, E., Silagadze, T., Smit, A.B., Stefansson, H., Steinberg, S., Suvisaari, J., Tosato, S., Verhage, M., Walters, J.T., Levinson, D.F., Gejman, P.V., Kendler, K.S., Laurent, C., Mowry, B.J., O'Donovan, M.C., Owen, M.J., Pulver, A.E., Riley, B.P., Schwab, S.G., Wildenauer, D.B., Dudbridge, F., Holmans, P., Shi, J., Albus, M., Alexander, M., Campion, D., Cohen, D., Dikeos, D., Duan, J., Eichhammer, P., Godard, S., Hansen, M., Lerer, F.B., Liang, K.Y., Maier, W., Mallet, J., Nertney, D.A., Nestadt, G., Norton, N., O'Neill, F.A., Papadimitriou, G.N., Ribble, R., Sanders, A.R., Silverman, J.M., Walsh, D., Williams, N.M., Wormley, B., Arranz, M.J., Bakker, S., Bender, S., Bramon, E., Collier, D., Crespo-Facorro, B., Hall, J., Iyegbe, C., Jablensky, A., Kahn, R.S., Kalaydjieva, L., Lawrie, S., Lewis, C.M., Lin, K., Linszen, D.H., Mata, I., McIntosh, A., Murray, R.M., Ophoff, R.A., Powell, J., Rujescu, D., Van Os, J., Walshe, M., Weisbrod, M., Wiersma, D., Donnelly, P., Barroso, I., Blackwell, J.M., Bramon, E., Brown, M.A., Casas, J.P., Corvin, A.P., Deloukas, P., Duncanson, A., Jankowski, J., Markus, H.S., Mathew, C.G., Palmer, C.N., Plomin, R., Rautanen, A., Sawcer, S.J., Trembath, R.C., Viswanathan, A.C., Wood, N.W., Spencer, C.C., Band, G., Bellenguez, C., Freeman, C., Hellenthal, G., Giannoulatou, E., Pirinen, M., Pearson, R.D., Strange, A., Su, Z., Vukcevic, D., Donnelly, P., Langford, C., Hunt, S.E., Edkins, S., Gwilliam, R., Blackburn, H., Bumpstead, S.J., Dronov, S., Gillman, M., Gray, E., Hammond, N., Jayakumar, A., McCann, O.T., Liddle, J., Potter, S.C., Ravindrarajah, R., Ricketts, M., Tashakkori-Ghanbaria, A., Waller, M.J., Weston, P., Widaa, S., Whittaker, P., Barroso, I., Deloukas, P., Mathew, C.G., Blackwell, J.M., Brown, M.A., Corvin, A.P., McCarthy, M.I., Spencer, C.C., Bramon, E., Corvin, A.P., O'Donovan, M.C., Stefansson, K., Scolnick, E., Purcell, S., McCarroll, S.A., Sklar, P., Hultman, C.M., Sullivan, P.F.Wellcome Trust Case Control, C., 2013. Genome-wide association analysis identifies 13 new risk loci for schizophrenia. Nat. Genet. 45, 1150–1159.

Sanders, A.R., Drigalenko, E.I., Duan, J., Moy, W., Freda, J., Goring, H.H.H., Gejman, P.V., 2017. Transcriptome sequencing study implicates immune-related genes differentially expressed in schizophrenia: new data and a meta-analysis. Transl. Psychiatry 7, e1093.

Schizophrenia Working Group of the Psychiatric Genomics, C., 2014. Biological insights from 108 schizophrenia-associated genetic loci. Nature 511, 421–427.

Schoretsanitis, G., Haen, E., Hiemke, C., Grunder, G., Stegmann, B., Schruers, K.R., Veselinovic, T., Lammertz, S.E., Paulzen, M., 2016. Risperidone-induced extrapyramidal side effects: is the need for anticholinergics the consequence of high plasma concentrations? Int. Clin. Psychopharmacol. 31, 259–264.

Sommer, I.E., Arango, C., 2017. Moving interventions from after to before diagnosis. World Psychiatry 16, 275–276.

Sommer, I.E., Bearden, C.E., van Dellen, E., Breetvelt, E.J., Duijff, S.N., Maijer, K., van Amelsvoort, T., de Haan, L., Gur, R.E., Arango, C., Diaz-Caneja, C.M., Vinkers, C.H., Vorstman, J.A., 2016. Early interventions in risk groups for schizophrenia: what are we waiting for? NPJ Schizophr. 2, 16003.

Stoodley, C.J., Valera, E.M., Schmahmann, J.D., 2012. Functional topography of the cerebellum for motor and cognitive tasks: an fMRI study. NeuroImage 59, 1560–1570.

Sugino, H., Futamura, T., Mitsumoto, Y., Maeda, K., Marunaka, Y., 2009. Atypical antipsychotics suppress production of proinflammatory cytokines and up-regulate interleukin-10 in lipopolysaccharide-treated mice. Prog. Neuro-Psychopharmacol. Biol. Psychiatry 33, 303–307.

Takahashi, T., Zhou, S.Y., Nakamura, K., Tanino, R., Furuichi, A., Kido, M., Kawasaki, Y., Noguchi, K., Seto, H., Kurachi, M., Suzuki, M., 2011. Longitudinal volume changes of the pituitary gland in patients with schizotypal disorder and first-episode schizophrenia. Prog. Neuro-Psychopharmacol. Biol. Psychiatry 35, 177–183.

Tamminga, C.A., Thaker, G.K., Buchanan, R., Kirkpatrick, B., Alphs, L.D., Chase, T.N., Carpenter, W.T., 1992. Limbic system abnormalities identified in schizophrenia using positron emission tomography with fluorodeoxyglucose and neocortical alterations with deficit syndrome. Arch. Gen. Psychiatry 49, 522–530.

Turgeon, S.M., Kegel, G., Davis, M.M., 2001. Electrolytic lesions of the medial septum enhance latent inhibition in a conditioned taste aversion paradigm. Brain Res. 890, 333–337.

Tustison, N.J., Avants, B.B., Cook, P.A., Zheng, Y., Egan, A., Yushkevich, P.A., Gee, J.C., 2010. N4ITK: improved N3 bias correction. IEEE Trans. Med. Imaging 29, 1310–1320.

Valdes-Hernandez, P.A., Sumiyoshi, A., Nonaka, H., Haga, R., Aubert-Vasquez, E., Ogawa, T., Iturria-Medina, Y., Riera, J.J., Kawashima, R., 2011. An in vivo MRI template set for morphometry, tissue segmentation, and fMRI localization in rats. Front Neuroinf. 5, 26.

van Erp, T.G., Hibar, D.P., Rasmussen, J.M., Glahn, D.C., Pearlson, G.D., Andreassen, O.A., Agartz, I., Westlye, L.T., Haukvik, U.K., Dale, A.M., Melle, I., Hartberg, C.B., Gruber, O., Kraemer, B., Zilles, D., Donohoe, G., Kelly, S., McDonald, C., Morris, D.W., Cannon, D.M., Corvin, A., Machielsen, M.W., Koenders, L., de Haan, L., Veltman, D.J., Satterthwaite, T.D., Wolf, D.H., Gur, R.C., Gur, R.E., Potkin, S.G., Mathalon, D.H., Mueller, B.A., Preda, A., Macciardi, F., Ehrlich, S., Walton, E., Hass, J., Calhoun, V.D., Bockholt, H.J., Sponheim, S.R., Shoemaker, J.M., van Haren, N.E., Pol, H.E., Ophoff, R.A., Kahn, R.S., Roiz-Santianez, R., Crespo-Facorro, B., Wang, L., Alpert, K.I., Jonsson, E.G., Dimitrova, R., Bois, C., Whalley, H.C., McIntosh, A.M., Lawrie, S.M., Hashimoto, R., Thompson, P.M., Turner, J.A., 2016. Subcortical brain volume abnormalities in 2028 individuals with schizophrenia and 2540 healthy controls via the ENIGMA consortium. Mole. Psychiatry 21, 585.

van Os, J., Rutten, B.P., Myin-Germeys, I., Delespaul, P., Viechtbauer, W., van Zelst, C., Bruggeman, R., Reininghaus, U., Morgan, C., Murray, R.M., Di Forti, M., McGuire, P., Valmaggia, L.R., Kempton, M.J., Gayer-Anderson, C., Hubbard, K., Beards, S., Stilo, S.A., Onyejiaka, A., Bourque, F., Modinos, G., Tognin, S., Calem, M., O'Donovan, M.C., Owen, M.J., Holmans, P., Williams, N., Craddock, N., Richards, A., Humphreys, I., Meyer-Lindenberg, A., Leweke, F.M., Tost, H., Akdeniz, C., Rohleder, C., Bumb, J.M., Schwarz, E., Alptekin, K., Ucok, A., Saka, M.C., Atbasoglu, E.C., Guloksuz, S., Gumus-Akay, G., Cihan, B., Karadag, H., Soygur, H., Cankurtaran, E.S., Ulusoy, S., Akdede, B., Binbay, T., Ayer, A., Noyan, H., Karadayi, G., Akturan, E., Ulas, H., Arango, C., Parellada, M., Bernardo, M., Sanjuan, J., Bobes, J., Arrojo, M., Santos, J.L., Cuadrado, P., Rodriguez Solano, J.J., Carracedo, A., Garcia Bernardo, E., Roldan, L., Lopez, G., Cabrera, B., Cruz, S., Diaz Mesa, E.M., Pouso, M., Jimenez, E., Sanchez, T., Rapado, M., Gonzalez, E., Martinez, C., Sanchez, E., Olmeda, M.S., de Haan, L., Velthorst, E., van der Gaag, M., Selten, J.P., van Dam, D., van der Ven, E., van der Meer, F., Messchaert, E., Kraan, T., Burger, N., Leboyer, M., Szoke, A., Schurhoff, F., Llorca, P.M., Jamain, S., Tortelli, A., Frijda, F., Vilain, J., Galliot, A.M., Baudin, G., Ferchiou, A., Richard, J.R., Bulzacka, E., Charpeaud, T., Tronche, A.M., De Hert, M., van Winkel, R., Decoster, J., Derom, C., Thiery, E., Stefanis, N.C., Sachs, G., Aschauer, H., Lasser, I., Winklbaur, B., Schlogelhofer, M., Riecher-Rossler, A., Borgwardt, S., Walter, A., Harrisberger, F., Smieskova, R., Rapp, C., Ittig, S., Soguel-dit-Piquard, F., Studerus, E., Klosterkotter, J., Ruhrmann, S., Paruch, J., Julkowski, D., Hilboll, D., Sham, P.C., Cherny, S.S., Chen, E.Y., Campbell, D.D., Li, M., Romeo-Casabona, C.M., Emaldi Cirion, A., Urruela Mora, A., Jones, P., Kirkbride, J., Cannon, M., Rujescu, D., Tarricone, I., Berardi, D., Bonora, E., Seri, M., Marcacci, T., Chiri, L., Chierzi, F., Storbini, V., Braca, M., Minenna, M.G., Donegani, I., Fioritti, A., La Barbera, D., La Cascia, C.E., Mule, A., Sideli, L., Sartorio, R., Ferraro, L., Tripoli, G., Seminerio, F., Marinaro, A.M., McGorry, P., Nelson, B., Amminger, G.P., Pantelis, C., Menezes, P.R., Del-Ben, C.M., Gallo Tenan, S.H., Shuhama, R., Ruggeri, M., Tosato, S., Lasalvia, A., Bonetto, C., Ira, E., Nordentoft, M., Krebs, M.O., Barrantes-Vidal, N., Cristobal, P., Kwapil, T.R., Brietzke, E., Bressan, R.A., Gadelha, A., Maric, N.P., Andric, S., Mihaljevic, M., Mirjanic, T., 2014. Identifying gene-environment interactions in schizophrenia: contemporary challenges for integrated, large-scale investigations. Schizophr. Bull. 40, 729–736.

Vitiello, B., Correll, C., van Zwieten-Boot, B., Zuddas, A., Parellada, M., Arango, C., 2009. Antipsychotics in children and adolescents: increasing use, evidence for efficacy and safety concerns. Eur. Neuropsychopharmacol. 19, 629–635.

Volkow, N.D., Wolf, A.P., Van Gelder, P., Brodie, J.D., Overall, J.E., Cancro, R., Gomez-Mont, F., 1987. Phenomenological correlates of metabolic activity in 18 patients with chronic schizophrenia. Am. J. Psychiatry 144, 151–158.

Yung, A.R., 2017. Treatment of people at ultra-high risk for psychosis. World Psychiatry 16, 207–208.